NOAA Technical Report NOS OES 001

TRANSPORT OF FINE PARTICULATES DISCHARGED AT THE 106-MILE MUNICIPAL SEWAGE SLUDGE DUMPSITE

Rockville, Maryland
October 1992

noaa National Oceanic and Atmospheric Administration

U.S. DEPARTMENT OF COMMERCE
National Ocean Service

Office of Ocean and Earth Science
National Ocean Service
National Oceanic and Atmospheric Administration
U.S. Department of Commerce

The Office of Ocean and Earth Sciences provides for the understanding of the coastal and ocean environment through the conduct of applied research and development in geophysics; the measurement, analyses, and product development of ocean and lake water levels; the collection, analyses, product development, and dissemination of coastal and global marine data; and the synthesis and interpretation with numerical and mechanistic modeling of global marine data sets. The Office cooperates with the U.S. Navy in conducting oceanographic activities for defense and mixed defense-civil sector purposes and applications.

It plans, develops and coordinates NOAA participation in Federally conducted oceanographic programs and activities, and facilitates cooperative programs, projects and activities with the oceanographic research community. It monitors and analyzes oceanographic activities between NOAA and other organizations and agencies; identifies potential conflicts, overlaps, and opportunities for joint or cooperative efforts; and develops and maintains cooperative agreements, Memoranda of Understanding and other arrangements as appropriate to resolve issues and to ensure maximum benefits from programs of mutual interest. It develops and maintains inventories of oceanographic programs, projects, systems and activities of other organizations and agencies to provide a basis for integrating current and future programs, systems and activities to ensure maximum efficiency and effectiveness in meeting national goals and requirements. The Office conducts research and development; carries out theoretical studies, data analyses, and engineering development; and formulates and executes programs encompassing technological development and application to oceanography, geophysics, geodesy, and related fields .

For the Great Lakes, coastal estuaries, sea coast and oceans, the Office plans, develops, and applies numerical and mechanistic models and produces predictions, forecasts, and analysis guidance materials of oceanographic and related marine meteorological phenomena; collects, analyzes and disseminates tide and water-level observations and associated information; and computes water-level datums for hydrographic, marine boundary and other special surveys. It evaluates and improves methods of data analysis; compares and integrates existing and new classes of data and products; provides and quality controls data sets and an array of output products; and assures science and technology transfer to and from the Office's programs and projects. The Office produces and disseminates operational marine environmental forecast and analysis guidance materials; manages and supports ocean climate studies; installs and operates real-time marine data collection systems; and formulates requirements for marine data sets and for data processing and communications systems; and designs and manages computer-based systems in support of these requirements.

NOAA Technical Report NOS OES 001

TRANSPORT OF FINE PARTICULATES DISCHARGED AT THE 106-MILE MUNICIPAL SEWAGE SLUDGE DUMPSITE

James H. Churchill
and
Frank Aikman, III

Rockville, Maryland
November 1992

United States
Department of Commerce
Barbara Hackman Franklin, Secretary

National Oceanic and
Atmospheric Administration
John A. Knauss, Under Secretary

National Ocean Service
W. Stanley Wilson
Assistant Administrator

NOTICE

Mention of a commercial company or product does not constitute an endorsement by NOAA. Use for publicity or advertising purposes of information from this publication concerning proprietary products or the tests of such products is not authorized.

TABLE OF CONTENTS

LIST OF FIGURES

LIST OF TABLES

ABSTRACT

The 106-Mile Municipal Sewage Sludge Dump Site (106-Mile Site) is located over the continental slope roughly 190 km east of the New Jersey coast. A critical issue regarding fine-grained sludge discharged at this site is whether or not it is carried to the shelf region in significant quantities. Numerous hydrographic sections and current meter data from recent field programs have shown that slope water, which typically occupies the 106-Mile Site, often intrudes into the shelf water mass in relatively thin layers at depths greater than 20 m. Using statistical models and current meter data from a number of large-scale field projects, it was found that a fraction of the material released at the 106-Mile Site may be transported to the shelf within the first 10 days after its discharge. In agreement with the hydrographic observations cited above, the onshelf flux of this material was found to be maximum between depths of 20–40 m during the summer season. However, points on the shelf are expected to be visited very infrequently by sludge within 10 days after its discharge from the 106-Mile Site: about 1 % of the time at the shelf edge and 0.01 % of the time 12 km shoreward. Furthermore, only a small fraction of the sludge released at the site, order $1°/_{oo}$, is expected to reside over the shelf. Calculations have also shown that heavy metal concentrations in sludge from the 106-Mile Site should not be distinguishable from background concentrations at locations over the shelf and upper slope.

1. INTRODUCTION

The 106-Mile Deep Water Municipal Sewage Sludge Dump Site (106-Mile Site) is situated over the continental slope, at water depths from 2200 to 2700 m, roughly 190 km east of southern New Jersey (Figure 1). In 1986 this site became an authorized disposal area for sewage sludge from New Jersey and the metropolitan area of New York City. By 1988 it received roughly 7×10^5 wet tons of sludge per month. Concerns over the environmental effects of this discharge helped lead to the passage of the Ocean Dumping Ban Act of 1988. This act barred marine disposal of sludge and industrial wastes after 31 December 1991 except through a compliance agreement with government agencies. It also required that a monitoring and research program be carried out to investigate the potential effect of sludge discharged at the 106-Mile Site.

The study described here was funded by NOAA as part of this program. It deals with the impact of fine-grained, slowly settling sludge particles. Specific questions considered are: At what frequency are points over the continental shelf and upper slope expected to receive material released at the 106-Mile Site? What fraction of sludge discharged at the 106-Mile Site makes it way to the continental shelf? What is the effect of dumping on heavy metal concentrations in near-surface waters?

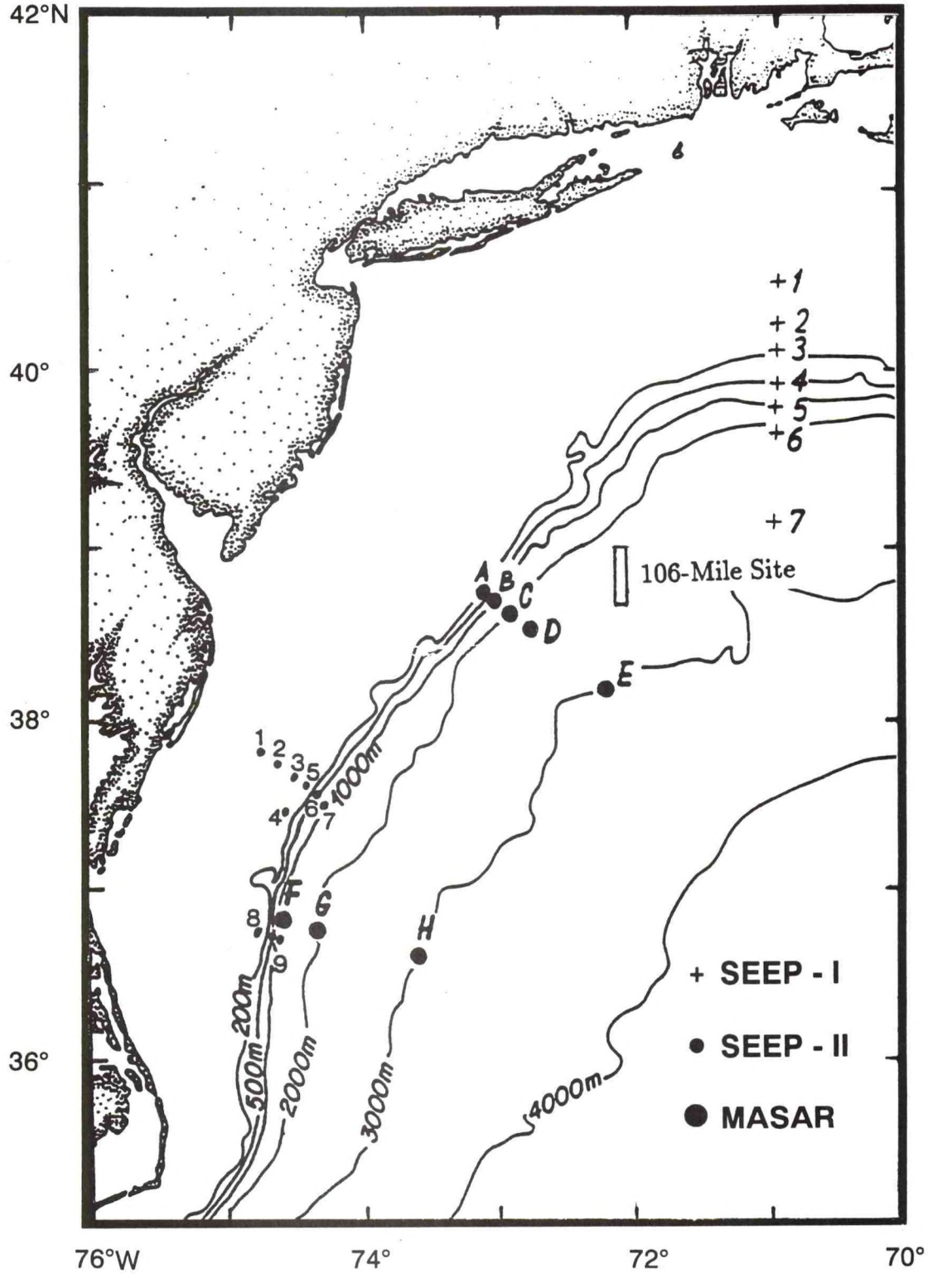

Figure 1. The Middle Atlantic Bight. The 106-Mile Dumpsite is indicated together with locations of moorings deployed in the SEEP-I, SEEP-II, and MASAR projects.

In dealing with these questions moored current meter data from a number of large-scale field projects are used to simulate the movement of water from the 106-Mile Site. Statistical concepts derived by Csanady (1983) and Churchill (1987) to quantify the impact of contaminants discharged from a fixed source are also employed. Their methodology required considerable modification for use in this study, because sludge is introduced to the 106-Mile Site from a moving rather than a fixed source. The revised formulae are presented and explained in the main body of the report. Details of their derivation are given in Appendices 1, 2 and 3.

In addition to addressing the above questions, this report also gives a brief review of what is currently known about water properties and currents off the northeast U. S. coast. This is presented first (Section 2) followed by a description of the statistical methods and data employed (Section 3). Details and results of the statistical analyses are then presented (Sections 4–7) followed by conclusions (Section 8).

2. REVIEW OF RELEVANT OCEANOGRAPHIC OBSERVATIONS

The 106-Mile Site lies within an oceanographic region referred to as the Middle Atlantic Bight (MAB) which extends from the southwest border of Georges Bank to Cape Hatteras (Figure 1). Understanding issues related to the transport of sludge from the 106-Mile Site requires at least a rudimentary understanding of the dynamics of the MAB. Present knowledge regarding water properties, water mass exchange and currents within the MAB is briefly reviewed in this section.

2.1 Water Mass Properties

The MAB is occupied by two large water masses: "slope water" and MAB shelf water. The shelf water mass is situated between the shore and a surface to bottom salinity front at the shelf-edge (hereafter the shelf-edge front). It contains local river discharge but is primarily supplied by inflow from the Gulf of Maine and Georges Bank. Its long-term mean flow is to the southwest at a rate of about 5 cm s^{-1} (Bumpus, 1973; Beardsley *et al.*, 1976, 1985; Mayer *et al.*, 1979; Aikman *et al.*, 1988), which is thought to be part of a long bouyancy-driven coastal current originating along the southern coast of Greenland (Chapman and Beardsley, 1989). The slope water mass is located between the shelf-edge and Gulf Stream fronts. It spans a salinity range of roughly 35–36 psu and is formed by a mixture of Coastal Labrador Sea Water and North Atlantic Central Water (Csanady and Hamilton, 1988).

The character of the shelf-edge front and the vertical stratification of MAB shelf and slope water vary in a seasonal cycle which is well documented (e.g. Bigelow, 1933; Ketchum and Corwin, 1964; Lyne and Csanady, 1984; Beardsley *et al.*, 1985). From late autumn through winter, intense storms and convective motions due to surface cooling vertically mix shelf water to the bottom and slope water to depths of 50–150 m. During this time, hereafter called the "unstratified season", a temperature and density front coincides with the shelf-edge salinity front (Figure 2). Throughout the rest of the year, weather systems tend to be less intense and near-surface convective motions are relatively weak. A surface mixed layer 5–40 m deep and an underlying seasonal pycnocline are typically seen during this time, the "stratified season". The seasonal pycnocline generally extends across the shelf and slope in a nearly horizontal plane. However, a near-surface and a near-bottom density front are usually found above and below the pycnocline (Figure 3).

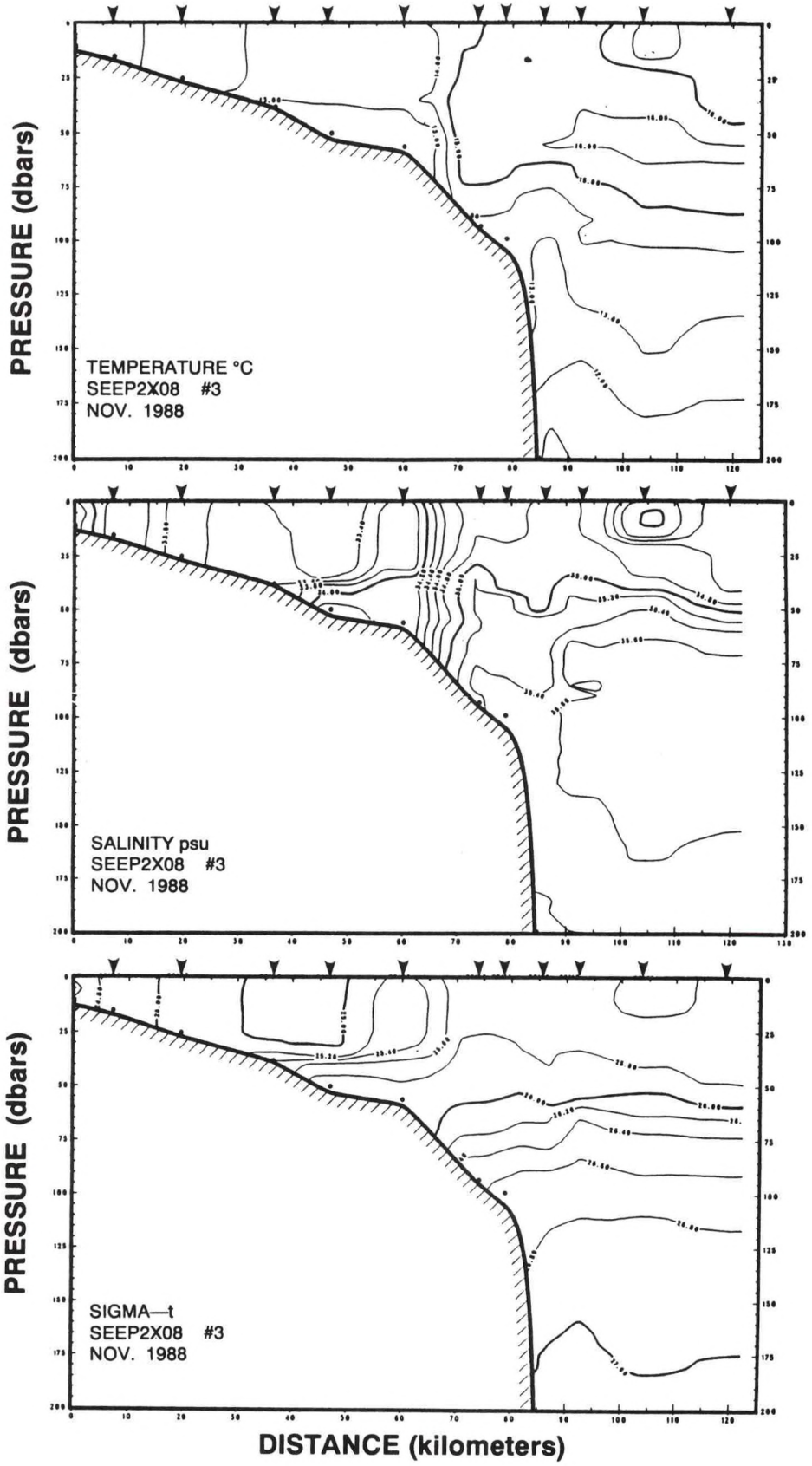

Figure 2. Distributions of temperature, salinity and sigma-t measured along the SEEP-II primary mooring line (formed by moorings 1, 2, 3, 4, 5, 6, and 7 shown in Figure 1) during November 1988.

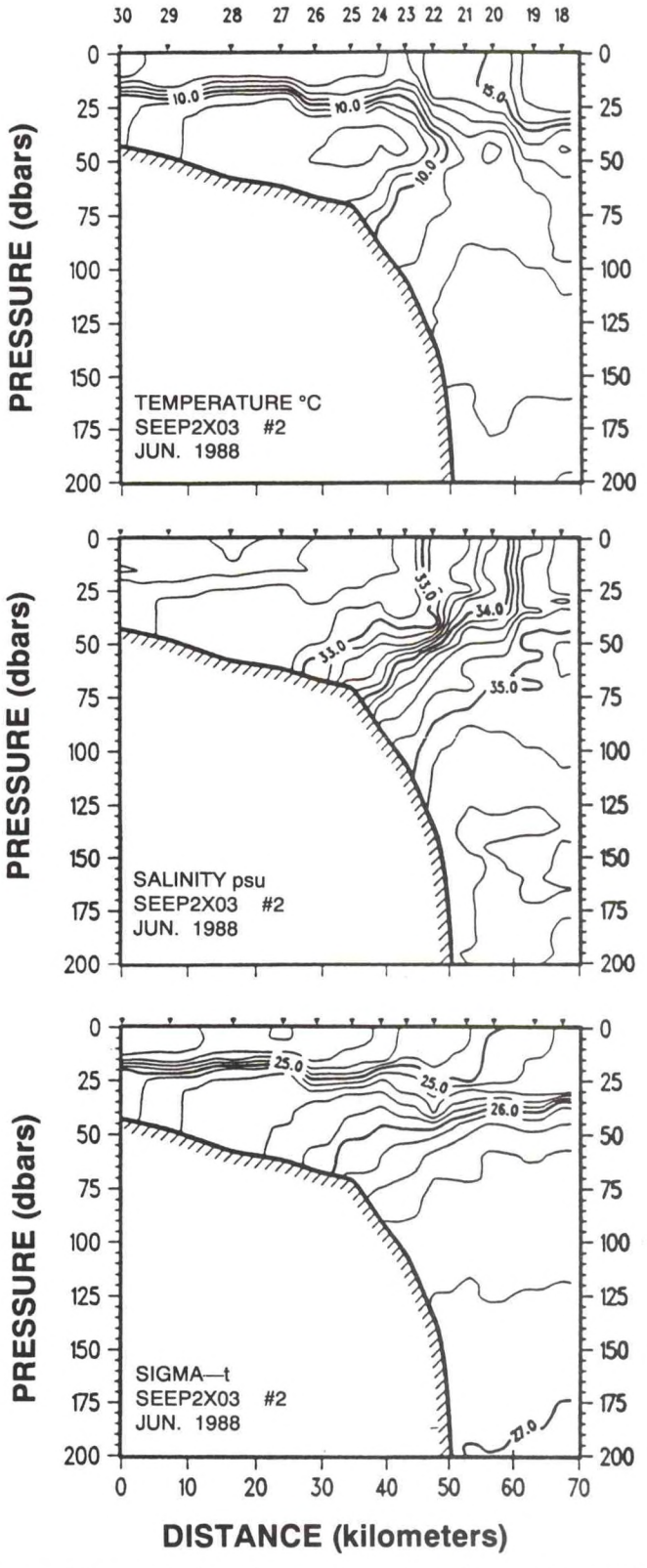

Figure 3. Same as Figure 2 except showing water properties measured in June 1988 (from Flagg *et al.*, 1992).

2.2 Slope Water Intrusions

The shelf-edge front is usually, but not always, shoreward of the 106-Mile Site. The transport of slope water onshore of the front is thus clearly of interest when considering the possibility that sludge from the 106-Mile Site makes its way to the continental shelf.

Intrusions of slope water shoreward of the front have often been observed in salinity sections derived from hydrographic data. During the stratified season, these intrusions usually take the form of a vertical salinity maximum within the pycnocline (Figure 4). These typically occur at depths between 10 and 40 m (Boicourt and Hacker, 1976; Gordon and Aikman, 1981; Houghton and Marra, 1983; Churchill *et al.*, 1986) and have been observed within 10 km of the coast (Churchill, 1985). Slope water intrusions seen during the unstratified season typically do not form a vertical salinity maximum and tend to occur at greater depths than in the stratified season, usually > 40 m. A slope water intrusion seen off Narragansett Bay during December 1979 is shown in Figure 5. This appeared beneath the surface 45 m and extended more than halfway across the shelf.

Only recently have velocity data been acquired within the MAB with vertical resolution sufficient to examine slope water intrusions. They came from Acoustic Doppler Current Profilers (ADCPs), instruments which sense water currents remotely by means of acoustic energy reflection off suspended particles. During 1988, ADCPs were deployed over the outer shelf and shelf-edge east of the Delmarva Peninsula (Figure 1) as part of the 2nd phase of the Shelf-Edge Exchange Processes project (hereafter, SEEP-II). These instruments gave velocity measurements at vertical intervals of 2–5 m over a range extending from 8 m off the bottom to 12 m below the surface.

Flagg *et al.* (1992) used the SEEP-II ADCP data to examine the formation of a slope water intrusion seen in the project's hydrographic data (shown here in Figure 4). They found that the intrusion was generated locally by cross-shelf currents within the SEEP-II region. They also found that this and other intrusions formed very rapidly, generally over a few days. The mechanism generating these was not apparent. Wind-forced circulation seemed to play a role in forming some intrusions but could not account for their full onshore extent.

Houghton *et al.* (1992) used SEEP-II data from an ADCP and a companion thermistor chain at the 90 m isobath to calculate cross-shelf heat fluxes throughout the water column. The time-averaged fluxes computed from data acquired in the stratified season agreed with the hydrographic observations of slope water intrusions cited above. These fluxes were of significant magnitude and directed onshore within the depth range typically occupied by the pycnocline (10-50 m).

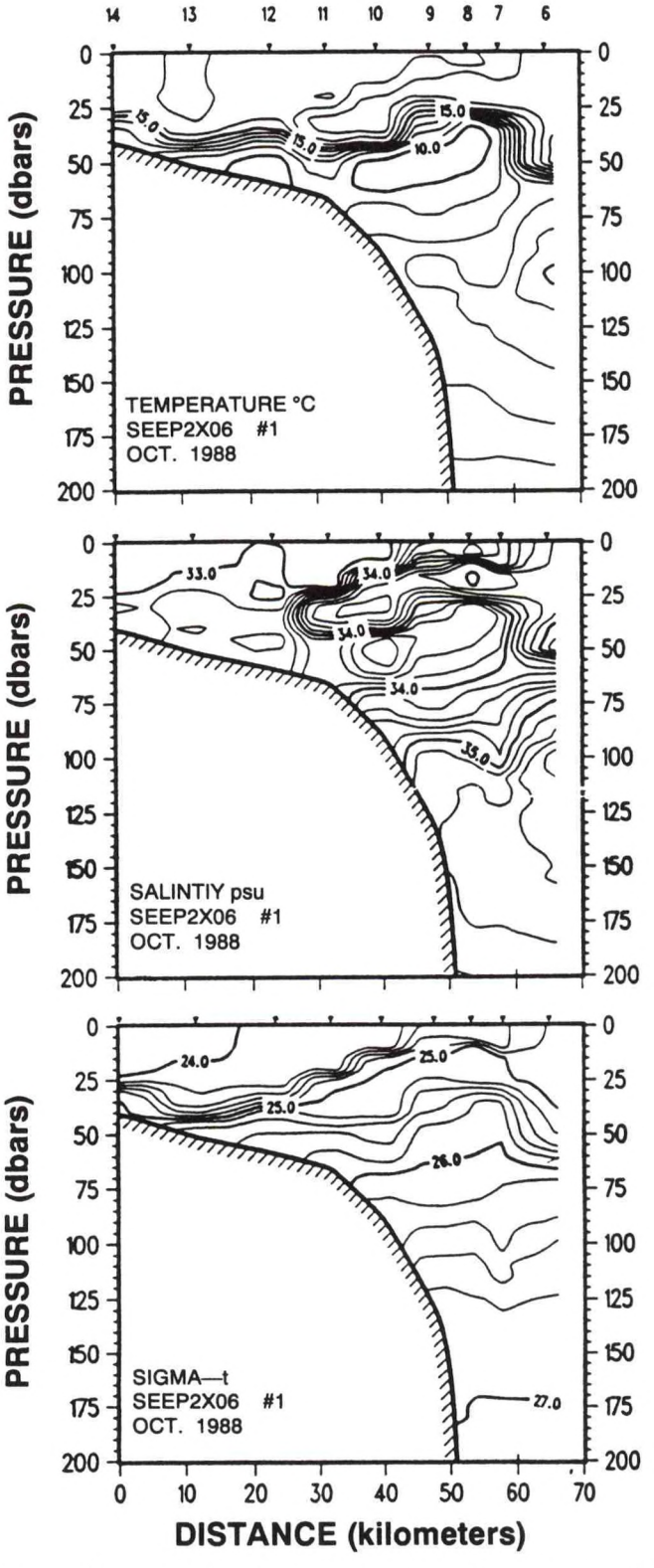

Figure 4. Same as Figure 2 except showing water properties measured in October 1988. The salinity section shows a mid-depth slope water intrusion extending onto the shelf as far as station 11.

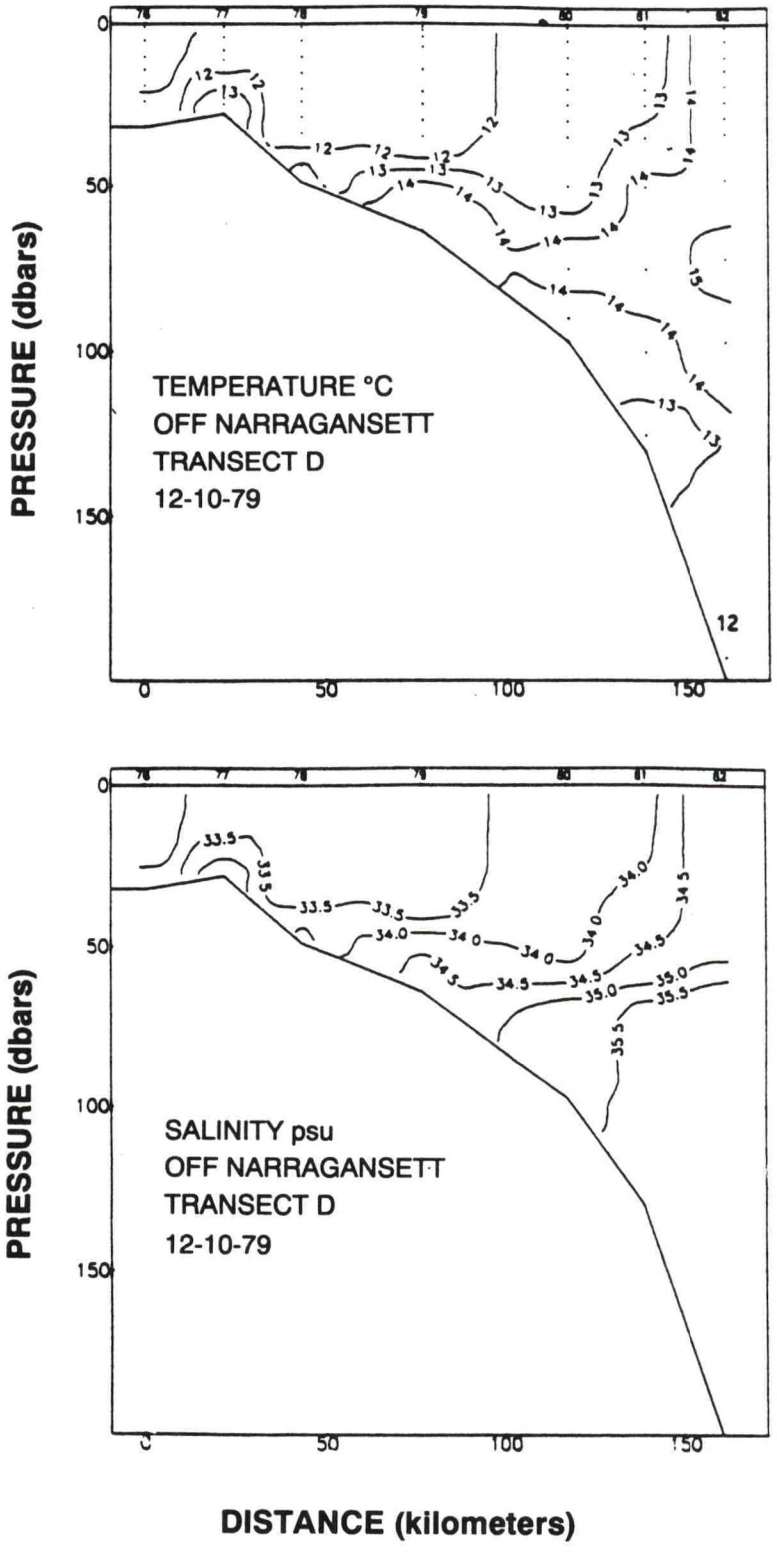

Figure 5. Distributions of temperature and salinity measured south of Narragansett Bay during December 1979 (from Manning and Holzwarth, 1990). The salinity section shows a near-bottom slope water intrusion extending to the 50 m isobath.

2.3. Gulf Stream Water Intrusions

Also of interest in this study are intrusions of Gulf Stream water into the slope water mass. The most thoroughly studied of these are Gulf Stream warm-core rings. These rings, which also contain Sargasso Sea water, are vigorous anticyclonic eddies with an initial diameter and maximum azimuthal velocity on the order of 150 km and 150 cm s^{-1}, respectively (Fornshell and Criess, 1979: Joyce, 1984; Joyce and Kennelly, 1985). They usually translate southwestward along the continental margin, but recombine with the Gulf Stream before reaching Cape Hatteras. A much less vigorous type of Gulf Stream water intrusion into MAB slope water has been identified by recent studies (Gawarkiewicz *et al.*, 1990; Churchill and Cornillon, 1991a,b). It consists of deep Gulf Stream water, which had upwelled along isopycnals before crossing the Gulf Stream front. Parcels of such water, hereafter referred to as discharged Gulf Stream water, are often observed in the slope region between Cape Hatteras and Hudson Canyon. These cover a relatively broad area (sometimes filling the entire region between the Gulf Stream front and the continental margin south of 38 °N) and encompass comparatively weak currents (generally <40 cm s^{-1}). This water does not appear to translate and is fairly long-lived, often remaining distinguishable in the sea surface temperature field for a number of weeks.

2.4. Slope Water Currents

Currents within MAB slope water were sampled by two large-scale moored instrument projects carried out in the 1980's. These are designated as the SEEP-I (Shelf-Edge Exchange Processes-I) and MASAR (Mid-Atlantic Slope and Rise) projects (see Figure 1 for mooring locations). Using data from these projects and published results of previous studies, Csanady and Hamilton (1988) devised a scheme for the circulation of slope water. Included in this scheme is a cyclonic current within the southern MAB consisting of a southwestward flow of 10-20 cm s^{-1} magnitude near the continental margin and a return northeastward flow adjacent to the Gulf Stream. More recent examination of the MASAR data set has shown that this current pattern is often shunted well to the north of Cape Hatteras by the discharged Gulf Stream water parcels described above (Churchill and Cornillon, 1991a,b). When such a parcel extends from the edge of the Gulf Stream to the shelf-edge (as is common), it sets up a pressure field which diverts the southwestward slope water flow over the continental slope to the east. The northern margin of the parcel then essentially becomes the southern terminus of the cyclonic slope water circulation.

Superimposed on the mean slope water circulation pattern are vigorous current fluctuations. Their general character is illustrated by Figure 6. This shows the principal axes and standard deviations along the axes of sub-tidal velocities measured at the MASAR moorings. These properties were derived from current meter records measured when warm-core rings were absent from the moorings and so truly represent velocity fluctuations of slope water. Two trends, which manifest the effect of the continental slope, stand out in

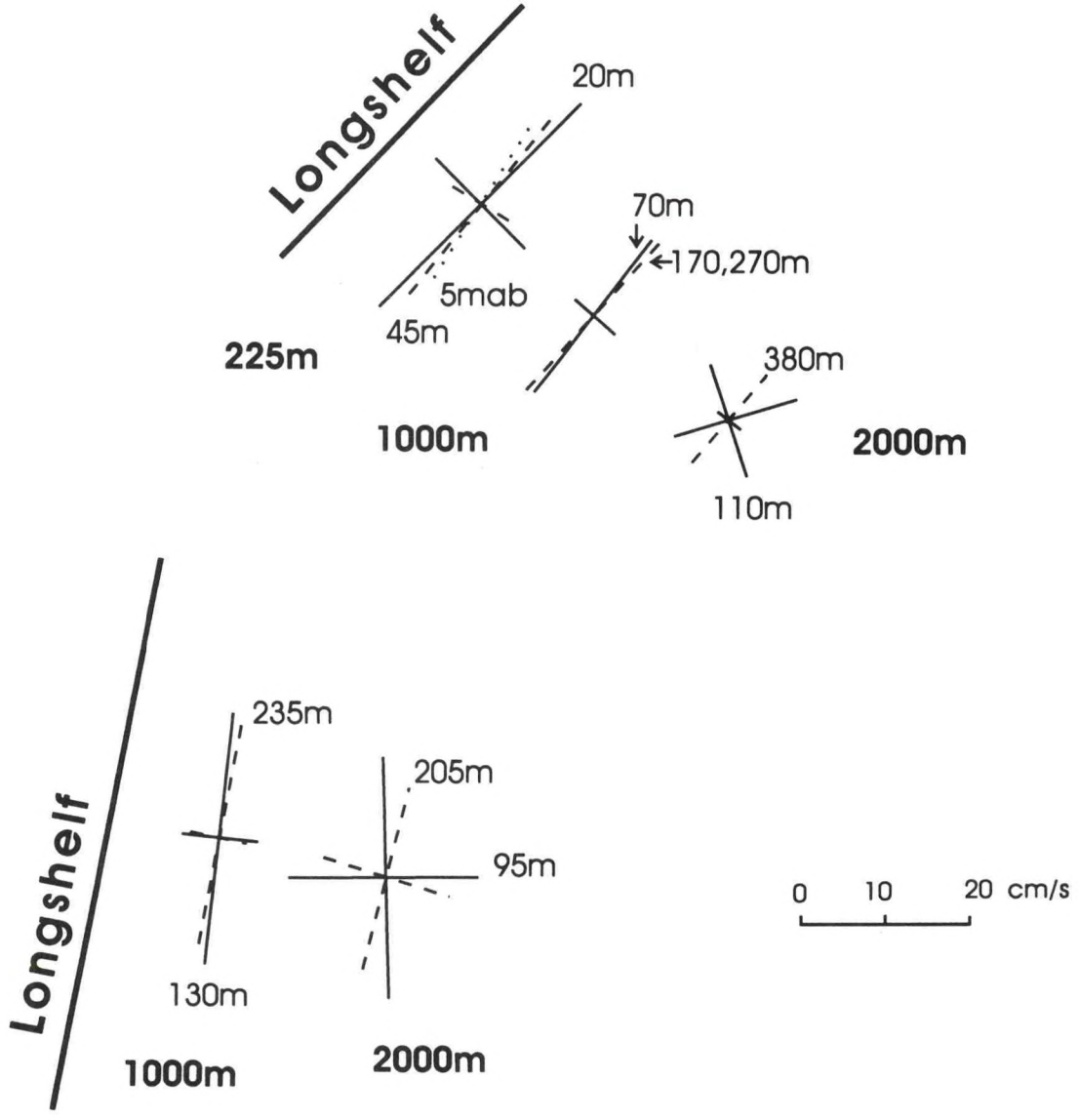

Figure 6. Principal axes of low-pass filtered currents measured within slope water by current meters deployed in the MASAR project. The length of each axis is proportional to the standard deviation of low-passed filtered velocity along the axis according to the scale shown. Dark/light numbers denote isobath/current meter depth. The approximate orientation of the shelf-edge at each mooring line is shown.

Figure 6. First, the major axes of the flow variations tend to be nearly aligned with the orientation of the continental margin, more so as the shelf-edge is approached. Second, the cross-slope velocity variance tends to decrease going towards the shelf-edge. Figure 6 also suggests that the statistical properties of slope water current fluctuations vary relatively little in the along-isobath direction.

Of critical concern to this study is the vertical structure of currents over the slope and shelf-edge. Unpublished analysis of MASAR current meter data by this author has revealed nearly slab-like flow over the slope between depths of 50 and 200 m. As an example, Table 1 gives the results of cross-spectral calculations relating subtidal currents measured at depths of 70 and 170 m at MASAR mooring B. In both the alongslope and cross-slope direction, the coherence of the currents at these levels is high (greatly exceeding the 95% significance level) and their transfer function has a magnitude and phase not appreciably different from one and zero, respectively. Similar results were obtained by Hamilton (1987) who analyzed currents measured at depths of 48, 95 and 248 m at a mooring deployed approximately 40 km southeast of the 106-Mile Site. Presentation of SEEP-II ADCP data by Flagg *et al.* (1992) revealed that, in contrast to slope water currents, currents over the MAB shelf-edge have a complex and varying vertical structure. In particular, the cross-shelf velocities measured at the shelf-edge by ADCPs during the summer of 1988 exhibited at least three different vertical structures: 2-layer, 3-layer and barotropic.

Many of the aspects of slope water circulation inferred from the moored current meter data have recently been confirmed by the tracks of near-surface drifters released within and near the 106-Mile Site as part of the EPA and NOAA funded 106-Mile Site research program. These drifters were tracked by system ARGOS. Each had a 7–7.5 m long holey sock drogue element centered at roughly 10 m depth. A total of 85 properly functioning drifters were released from October 1989 through October 1991. Their tracks clearly illustrate the cyclonic circulation pattern in slope water of the southern MAB (Battelle, 1991; Aikman and Empie, 1992). They also provide further evidence that this circulation is frequently blocked by discharged Gulf Stream water wedged between the continental margin and the Gulf Stream front north of Cape Hatteras (Figure 7).

TABLE 1

Results of cross-spectral calculations relating subtidal (periods>32 hr) velocity fluctuations measured at depths of 70 and 170 m at MASAR mooring B (Figure 1). The 95% significance level of coherence is 0.16. The confidence levels of transfer function phase and magnitude are at the 95% significance level.

		Transfer Function	
Component	Coherence	Magnitude	Phase
longshore	0.91	1.09 ± 0.08	2 ± 3°
cross-shore	0.72	0.97 ± 0.15	4 ± 6°

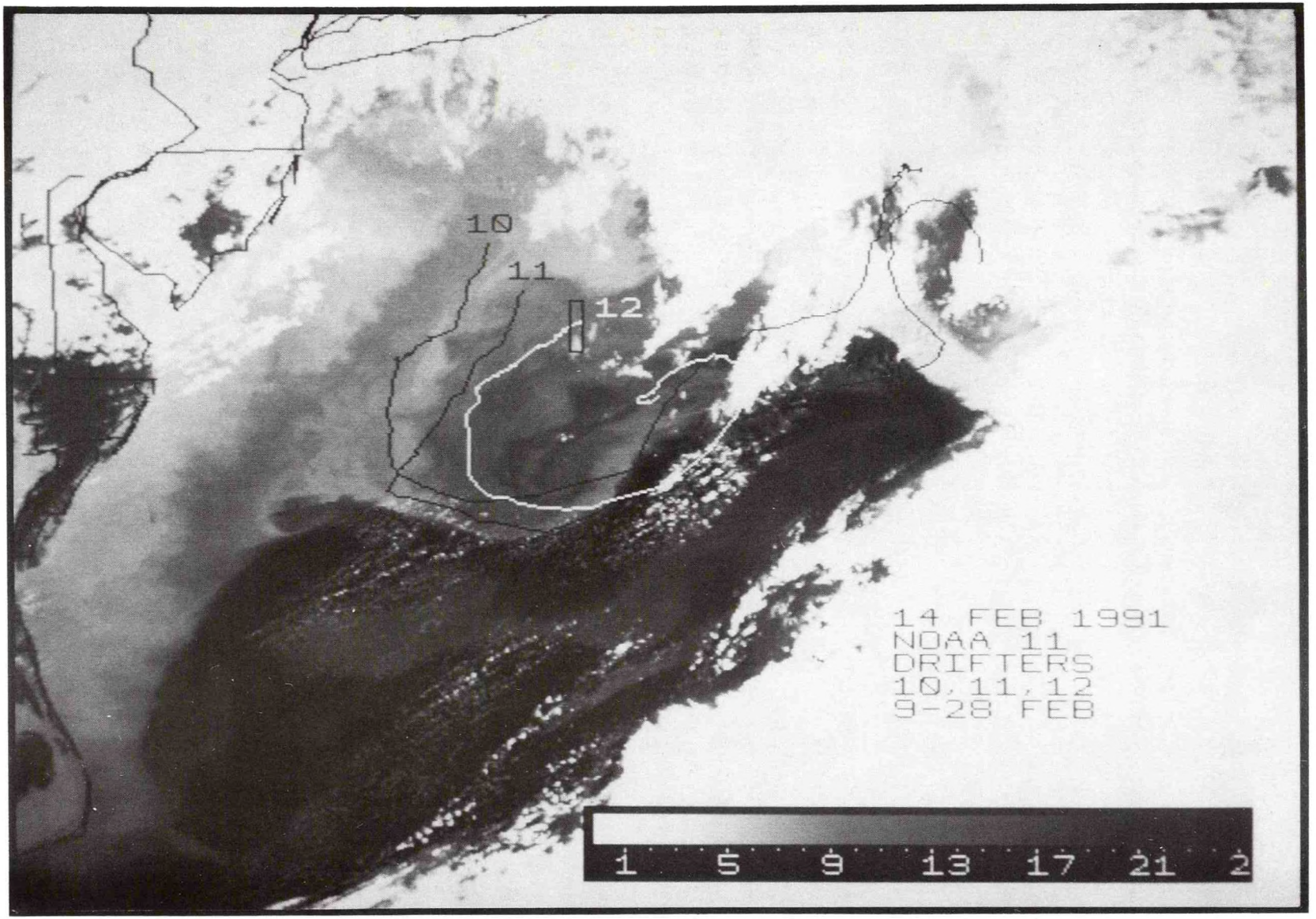

Figure 7. Satellite radiometer-derived image of sea surface temperature on 14 February 1991. Warmer water is progressively darker (scale at bottom right). A large mass of discharged Gulf Stream water (represented by nearly black tones) appears over the continental slope east of North Carolina and Virginia. Superimposed on the image are tracks followed by three drifters (numbered 10-12), drogued at 10 m depth, over the period 9-28 February 1992. The southwestward movement of all drifters is diverted to the east just to the north of the discharged Gulf Stream water mass.

3. STATISTICAL METHODS

3.1. Dispersal By Randomly Varying Currents

The statistical methods used here are based on the concept introduced by Csanady (1983) [hereafter, C83]. Csanady noted that the material released from a discrete contaminant source may be characterized by the elapsed time since its release, which he referred to as the material's "age". He proposed that the concentration field of such material may be divided into two parts. One is due to material of young age with a relatively high contaminant concentration, and the other is due to older, more diffuse, material. Mathematically, this separation may be expressed by:

$$C_T(x) = C(x, 0, T_D) + C(x, T_D, \infty) \quad (1)$$

where $C_T(x)$ is the total stochastic mean concentration at a point x of material discharged from a discrete source, $C(x, 0, T_D)$ is the mean concentration of discharged material arriving at x with an age less than T_D and $C(x, T_D, \infty)$ is the mean concentration of older discharged material which appears at x (here and throughout this report, x is a position vector made up of Cartesian components). In terms of the contaminant concentration history occurring at a site, $C(x, 0, T_D)$ may be thought of as the mean of the concentration spikes appearing when a concentrated plume emanating from the contaminant source is present at x, and $C(x, T_D, \infty)$ can be regarded as the underlying "background" concentration (given an appropriate choice of T_D). C83 noted that intermittent short-term exposure to the high contaminant concentration poses a special hazard to resident biota, different from that due to long-term exposure to the background concentration. To quantify this hazard he introduced a property termed the "visitation frequency", which is the stochastic mean proportion of time at which a site is immersed in discharged contaminants with an age less than some specified value. C83 developed a method to compute the visitation frequency field of a contaminant plume emanating from a fixed source. This method required that the water parcel excursions originating at the source be straight and that the plume width remain constant. It was thus valid for only short times since release, of order a few hours. Churchill (1987) developed a more generalized method for computing the visitation frequency field, allowing for meandering water parcel displacements and variation in plume width depending on plume element age.

The methodology developed by C83 and Churchill (1987) are applicable to a spatially fixed contaminant source only. However, contaminants are discharged from the 106-Mile Site from a moving source. Determining the visitation frequency of material set out from this type of source requires a different approach than that employed by C83 and Churchill (1987) because, unlike a fixed source, a moving one creates plume area at a rate proportional to its speed. Development of a visitation frequency formula applicable to a mobile contaminant discharge is carried out in Appendix 1. The result is:

$$\gamma(x, T_D) = \frac{I\,V}{A_S} \int_0^{T_D} w(t) \int\int_{\mathbf{A_S}} P(x_S, x, t) da_S dt \ . \qquad (2)$$

$\gamma(x, T_D)$ is the visitation frequency, i.e. the probability that discharged material arrive at x within an interval T_D after its release. $\mathbf{A_S}$ denotes the discharge region and A_S is its horizontal area. V is the average speed of the contaminant source. I is an indicator of the "intensity" of discharge operations. It is the average number of sources releasing material within $\mathbf{A_S}$ at one time (i.e., $I = 2$ for continuous discharge from two sources, or $I = 0.5$ if only one source is in operation half of the time). $w(t)$ is the typical cross-axial width of a plume element at a time t after its release. $P(x_S, x, t)$ is a probability density function such that $P(x_S, x, t)da$ is the likelihood that a passive tracer released at x_S be found at a time t after release in a region of area da with center point at x. In the expression above, $P(x_S, x, t)$ is integrated over all starting points, x_S, within the discharge region (da_S is a small area upon which x_S is centered).

Derived in Appendix 2 is the following expression for $C(x, 0, T_D)$ applicable to material released from a mobile discharge confined to a region $\mathbf{A_S}$:

$$C(x, 0, T_D) = \frac{m}{A_S D} \int_0^{T_D} F(t) \int\int_{\mathbf{A_S}} P(x_S, x, t) da_S dt \ . \qquad (3)$$

$C(x, 0, T_D)$ is as defined above with the added specification that it is the vertically-averaged concentration over a designated layer of thickness D. $F(t)$ is the fraction of discharged material of age t which typically resides in the layer. m is the average rate of discharge into $\mathbf{A_S}$ in units of mass per time. Note that $C(x, 0, T_D)$ does not depend on either V or $w(t)$. This is because an increase in discharge source speed or in the width of the resulting plume will increase the likelihood that the plume encounter a site, but will bring about a proportionate decrease in the concentration expected at an encounter.

3.2. Specification Of Parameters

The parameters and functions which must be specified in order to determine C and γ from the above expressions are dealt with below.

Characteristic Barge Speed - V

There are numerous reported measurements of barge speed during discharge at the 106-Mile Site. Those reviewed by this author (Battelle 1988a,b, 1989) range from 2.2 to 5.4 m s^{-1} and have a mean of approximately 3 m s^{-1}. Accordingly, V has been set to 3 m s^{-1}.

Initial Plume Width - $w(0)$

A number of field investigations of sludge plumes have been carried out within and near the 106-Mile Site (Battelle, 1988a,b, 1989, 1990; EA Engineering 1991). These have shown that turbulence generated by the barge wake acts to mix the discharged material vertically to a depth of roughly 20 m and horizontally over a width of approximately 100 m. Based on these observations, initial plume width, $w(0)$ was set to 100 m. The plume width subsequent to wake-induced mixing took on two definitions in this study. These are dealt with in Sections 4 and 5.

Intensity of Discharge - I

By definition, I may be expressed as

$$I = B(T)/T \tag{4}$$

where $B(T)$ is the cumulative time of single-source discharge (i.e., barge-hours) over a period T. $B(T)$ can be estimated as the ratio of the total sludge volume discharged, $L(T)$, to a characteristic dumping rate, l. This gives

$$I \simeq \frac{L(T)}{lT} \tag{5}$$

The total amount of sludge discharged at the 106-Mile Site is reported in "wet" weight and equals roughly 9×10^6 wet tons per year (Table 2). For a sludge density of 1.05 gm cm^{-3} this converts to $L(T)/T = 250$ l s^{-1}. In specifying l, it was necessary to chose between the average dumping rate of two periods. In August 1989 the average rate declined dramatically, roughly from 12000 to 3500 gal min^{-1}, due to a decrease in the maximum allowable dumping rate (Carlton Hunt, personal communication). In this analysis, consideration is given to the lower dumping rate only. Setting l to 3500 gal min^{-1} (225 l s^{-1}) and using the above value of $L(T)/T$ gives $L(T)/[l\ T] = 1.1$. Because this does not significantly differ from unity, I has been set to 1 in the calculations described below.

Average Mass Rate of Discharge - m

As part of this study (3) was evaluated to give the mean concentration field of heavy metals discharged at the 106-Mile Site. This required specifying the rate of heavy metal discharge. Measurements have shown that the heavy metal concentration in sludge prior to dumping varies considerably from district to district (Battelle, 1988c). Taking this into

account, the average rate at which a particular metal element was released at the 106-Mile Site was computed according to

$$m_k = \frac{1}{\rho\, T} \sum_{i=1}^{N} W_i(T) C_{Rik}(T) \qquad (6)$$

where k denotes a specified element, $W_i(T)$ is the wet weight of sludge discharged by district i over a period T, C_{Rik} is the mean concentration of element k in this material prior to discharge, and ρ is wet sludge density. The above has been evaluated for various heavy metals using ρ =1.05 gm cm^{-3}, reported $W_i(T)$ values for 1989-1990 (Table 2), and metal concentrations measured in sludge samples collected from all districts in August 1988 (Battelle, 1988c, Table 11). The results for lead and copper are: m_{Pb} =4.5 gm s^{-1} and m_{Cu} =10.1 gm s^{-1}.

Fraction of Material Retained in a Specified Layer - $F(t)$

The analysis to be described in Section 4 required estimation of $F(t)$ for a surface layer initially containing the entire sludge plume immediately after barge-wake-induced mixing (i.e. $F(0)$ =1). If the effect of heavy metals is at issue (as it is here), then it is reasonable to assume that the sludge plume is made up of particles only, as most (>95%) of the heavy metals in sludge are attached to particles (Carlton Hunt, personal communication). Loss of particulate sludge from a surface layer results from particle settling and vertical mixing. A number of processes may effect vertical mixing of near-surface waters. These include shear-induced turbulence, internal wave breaking and convective motions due to surface cooling. Unfortunately, the characteristic rate of mixing due to these processes can not be specified with confidence, especially for mixing during the unstratified season which is expected to be strong episodically, due to atmospheric storms or cold air outbreaks. For this reason, $F(t)$ was determined by considering particle settling only. The resulting function admittedly overestimates the expected fraction of material retained in a surface layer, because loss due to mixing is ignored. We feel it's better to err on the conservative side (i.e. overestimate the amount of sludge in the surface layer). In any case, the error is deemed acceptable when dealing with material contained within the surface mixed layer during the stratified season (because vertical mixing is suppressed at the pycnocline) or with material residing in a surface layer during the unstratified season if only short times since release are considered.

Estimation of $F(t)$ involved dividing sludge particles into a number of "settling classes" each containing a specified fraction of the sludge, G_j, with average settling rate of W_j. For a total of M classes, $F(t)$ was determined from

TABLE 2

Weights of sludge discharged in the MAB by year and permittee. 1988-1991 values are for discharge at the 106-Mile Site only. Values courtesy of Battelle Ocean Sciences Inc.

Permittee	1987[1]	1988	1989	1990	Jan-Jun 1991
Wet Tons BCUA	607,786.0	423,140.0	299,214.2	298,277.5	63,039.8
JMEUC	266,074.9	307,707.0	226,212.1	240,397.5	44,610.0
LRSA	93,381.0	74,000.0	48,251.0	47,397.2	13,675.8
MCUA	982,978.4	996,811.8	1,008,780.1	1,321,330.9	221,103.7
PVSC	1,212,384.0	1,354,693.9	1,621,705.4	1,840,985.1	316,393.4
RVSA	98,203.1	129,403.1	131,745.9	123,586.0	1,946.1
WCDEF	494,442.0	543,882.0	490,096.0	489,647.9	222,706.8
NCDPW	810,752.0	872,539.0	896,609.0	915,743.5	432,184.0
NYCDEP	3,860,420.0	4,243,698.0	3,952,364.0	4,636,979.0	2,166,843.0
Wet Tons Totals	8,426,421.4	8,945,874.8	8,674,977.7	9,914,344.6	3,482,502.6

Note[1] 1987 totals include combined DS-106 and 12-mi site totals

$$F(t) = \sum_{j=1}^{M} G_j f_j(t) \tag{7}$$

where $f_j(t)$ is the fraction of material of class, j, which is retained in the layer under consideration at time, t, after release. By assuming that sludge is mixed uniformly by the turbulence induced by the barge wake, $f_j(t)$ was computed from the following expression

$$\begin{aligned} f_j(t) &= 1 - W_j t/D \qquad && t \leq D/W_j \\ &= 0 && t > D/W_j \end{aligned} \tag{8}$$

where, as before, D is layer thickness.

In evaluating (7) and (8), f_j and W_j were specified using the settling velocity distribution of sludge from Middlesex, New Jersey measured by Lavelle *et al.* (1988). The same settling velocity distribution was employed by Fry and Butman (1991) in tracking coarse particles discharged at the 106-Mile Site.

$\underline{P(x_S, x, t)}$

Determination of $P(x_S, x, t)$ involves simulating fluid parcel tracks originating from an array of starting points, x_S, distributed over the discharge region, $\mathbf{A_S}$. The tracks from a particular starting point give ensembles of trajectory endpoints for various times since release. The density of the points in an ensemble approximate $P(x_S, x, t)$ for the given values of x_s and t. For example, consider the case in which n out of an ensemble of N endpoints, each terminating a trajectory starting at x_{Si} and of duration t_j, are found in a cell $\mathbf{a_k}$. The estimate of $P(x_{Si}, x_k, t_j)$ at a point x_k in $\mathbf{a_k}$ is $n/(Na_k)$. To obtain $\gamma(x_k, T_D)$ estimates of this type must be determined for a number of starting points over $\mathbf{A_S}$ and for a number of parcel excursion times from each point.

Simulating fluid parcel tracks originating at the 106-Mile Site was carried out using current meter data from three large-scale moored instrument projects: SEEP-I, SEEP-II and MASAR, which were discussed earlier. The current meters deployed in the SEEP-I and MASAR studies measured velocities at a single point. They were set out along three primary mooring lines, with most moorings located on the slope and rise (Figure 1). The SEEP-II project was carried out over the shelf and slope east of Virginia and was marked by a heavy concentration of instruments at the shelf-edge. As noted in Section 2, these included bottom-mounted ADCPs, which were set at the 60, 90 and 130 m isobaths.

In simulating fluid parcel tracks, a spatial velocity field was created with the current meter data. It was allowed to vary as a function of cross-isobath distance only (i.e., velocities were considered uniform in the along-isobath direction). Typically, the data from current

meters on a cross-isobath transect were employed. In such cases, the flow field was specified such that velocity varied linearly with cross-isobath distance between current meters and was spatially uniform seaward and shoreward of the transect.

Clearly, fluid tracks created as described above will deviate from actual tracks, more so with increasing tracking time. However, the intent here is not to mimic fluid trajectories, but to obtain a reasonable approximation of $P(x_S, x, t)$. Nevertheless, the question naturally arises as to whether P can be adequately estimated from moored current meter data. A detailed treatment of this question is beyond the scope of this paper, but a brief discussion of some of the primary issues is warranted

A concern raised by previous work is the error in the time scale of velocity fluctuations sensed by current meter data. Hay and Pasquill (1959) demonstrated that even if Eulerian measurements resolve a velocity field perfectly, the dispersion rate derived from these measurements may differ from the actual rate due to a mismatch between Eulerian and Lagrangian correlation time scales. They further postulated that time scales deduced from Eulerian measurements should be shorter than Lagrangian time scales because velocity fluctuations are advected past a fixed point sensor making them appear at a higher than actual frequency. This effect does not seem to introduce serious error in this study, however. Preliminary calculations by these authors and P. Dragos of Battelle Ocean Sciences using moored current meter and Argos drifter data reveal that Eulerian and Lagrangian time scales of currents over the MAB slope are comparable.

It can be shown from turbulent diffusion theory (see Csanady, 1980; and Hinze, 1975) that if Lagrangian and Eulerian velocity time scales nearly match, then a large number of independent fluid tracks derived from moored current meter data will yield P with reasonable certainty so long as these data resolve the "basic" velocity statistics in the region of interest. These basic statistics are mean velocity, principal axes orientation of velocity fluctuations and variances about the principal axes (or equivalently mean velocity and variance and covariance of velocity components). As noted in Section 2.3, the basic statistics of near-surface velocities over the MAB slope do not change significantly with depth and vary slowly going along isobaths. Current meter data from the SEEP-I and MASAR cross-slope transects should thus resolve these statistics with reasonable certainty over a fairly large area of the slope. Its longslope extent will be limited by the appearance of discharged Gulf Stream water parcels to the north of Cape Hatteras which, as noted in Section 2.3, tend to divert the southwestward slope water current near the continental margin to the east (see Figure 7). However, these parcels seldom extend to within 200 km of the 106-Mile Site (Churchill and Cornillon 1991a,b).

4. EFFECT OF HEAVY METALS

An issue of particular concern is the effect of heavy metals contained in sludge discharged at the 106-Mile Site. Two aspects of this issue have been examined as part of this study. These are: the impact of sewage dumping on the long-term mean concentration of heavy metals near the sea surface, and the range over which detectable concentrations of heavy metals are expected. Sample findings for lead only are presented here.

4.1. Contribution To The Mean Concentration Field

During the stratified season barge-wake-induced mixing distributes sludge discharged at the 106-Mile Site over most or all of the surface mixed layer depth (Battelle, 1988a, 1989). Considered here is the long-term mean concentration of discharged lead within the surface mixed layer during the stratified season. This was estimated from (3) with D=20 m, the approximate average surface mixed layer depth during the stratified season as judged from the hydrographic profiles presented by Lyne and Csanady (1984). $F(t)$ was determined by the method described in Section 3.2, and m_{Pb} was set to 4.5 g s^{-1} (Section 3.2). P was determined from fluid parcel tracks simulated using velocity data collected over the period 15 April–1 September 1984 from current meters set at 45–70 m depth on the MASAR northern mooring line. T_D was set to 10 days, which gave non-zero P over an area extending in the alongslope direction roughly from 40 km northeast to 200 km southwest of the 106-Mile Site. The resulting concentration field (Figure 8) does not exceed 25 ng/l (1 ng=10^{-9} g), the approximate "background" concentration of Pb in nearsurface slope water (Battelle, 1990), at points more than 40 km from the dumpsite. It also gives clear evidence that dumping at the 106-Mile Site should not appreciably affect mean lead concentrations over the upper slope and shelf-edge.

4.2. Range Of Detectable Concentrations

A property which can be determined by (2) is the frequency at which discharged material with a detectable contaminant concentration is expected to appear at a given site. This is estimated by specifying a minimum detectable contaminant concentration, C_B (relative to the background concentration), and defining $w(t)$ as the typical distance across the discharged plume axis with contaminant concentration in excess of C_B. The evolution of $w(t)$ defined in this manner is illustrated in Figure 9.

Following Churchill (1987), $w(t)$ defined as above can be estimated by assuming that contaminant concentration normal to the plume axis has a Gaussian form given by

$$C_P(\varepsilon,t) = \frac{Q\ F(t)}{\sqrt{2\pi}\sigma(t)}\exp[-\varepsilon^2/2\sigma^2(t)], \tag{9}$$

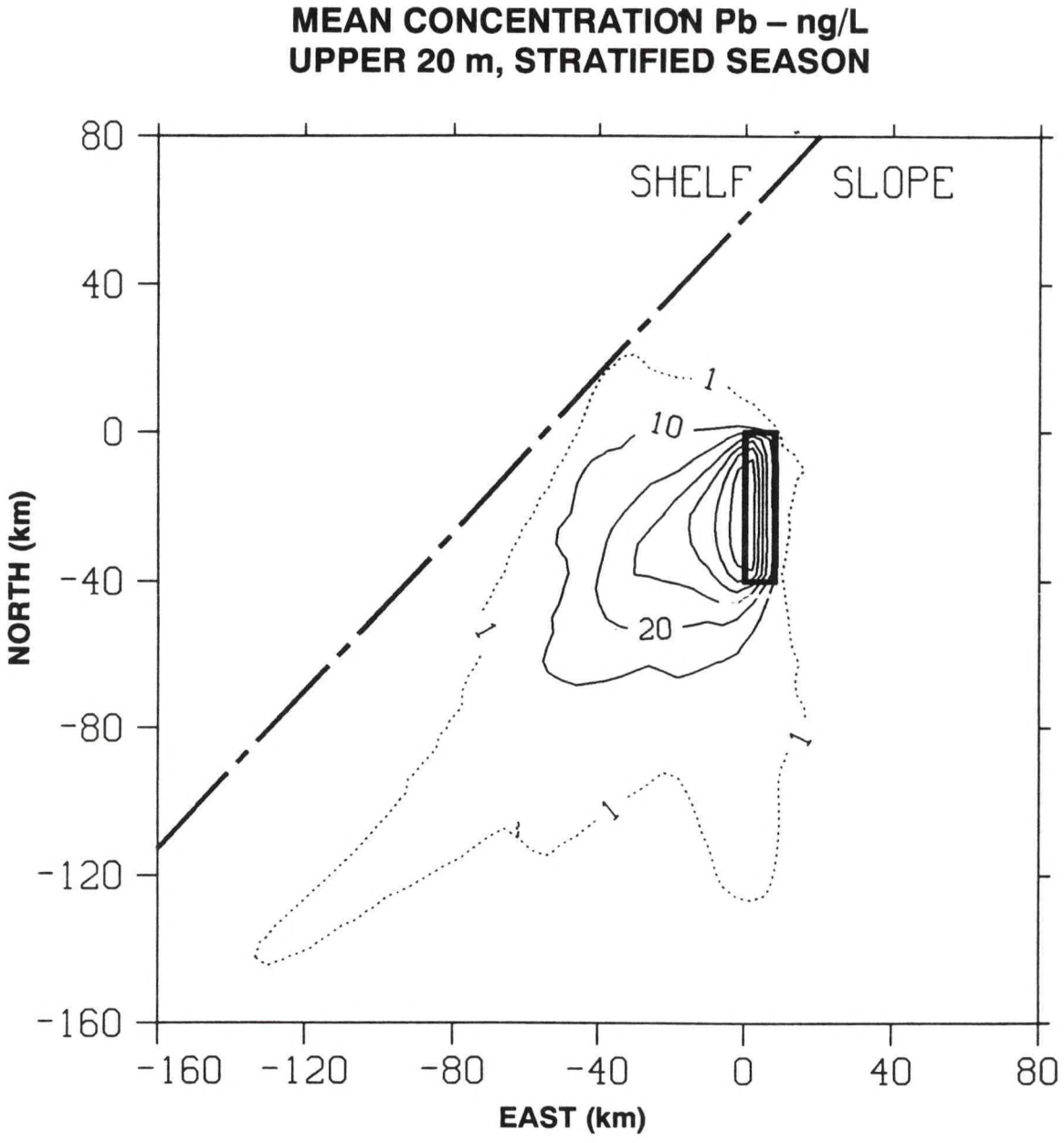

Figure 8. Estimated field of the stochastic mean concentration of discharged lead within the surface mixed layer during the stratified season. Concentrations were computed according to (3) with D=20 m and T_D=10 days, and using velocity data collected during the period of 15 April-1 September 1984 from current meters set at 45-70 m depth on MASAR moorings A, B, and E (Figure 1). The discharge area, 106-Mile Site, is the bold-line rectangle with its northwest corner at the coordinate system origin. The heavy broken line shows the approximate location of the shelf-edge (200 m isobath).

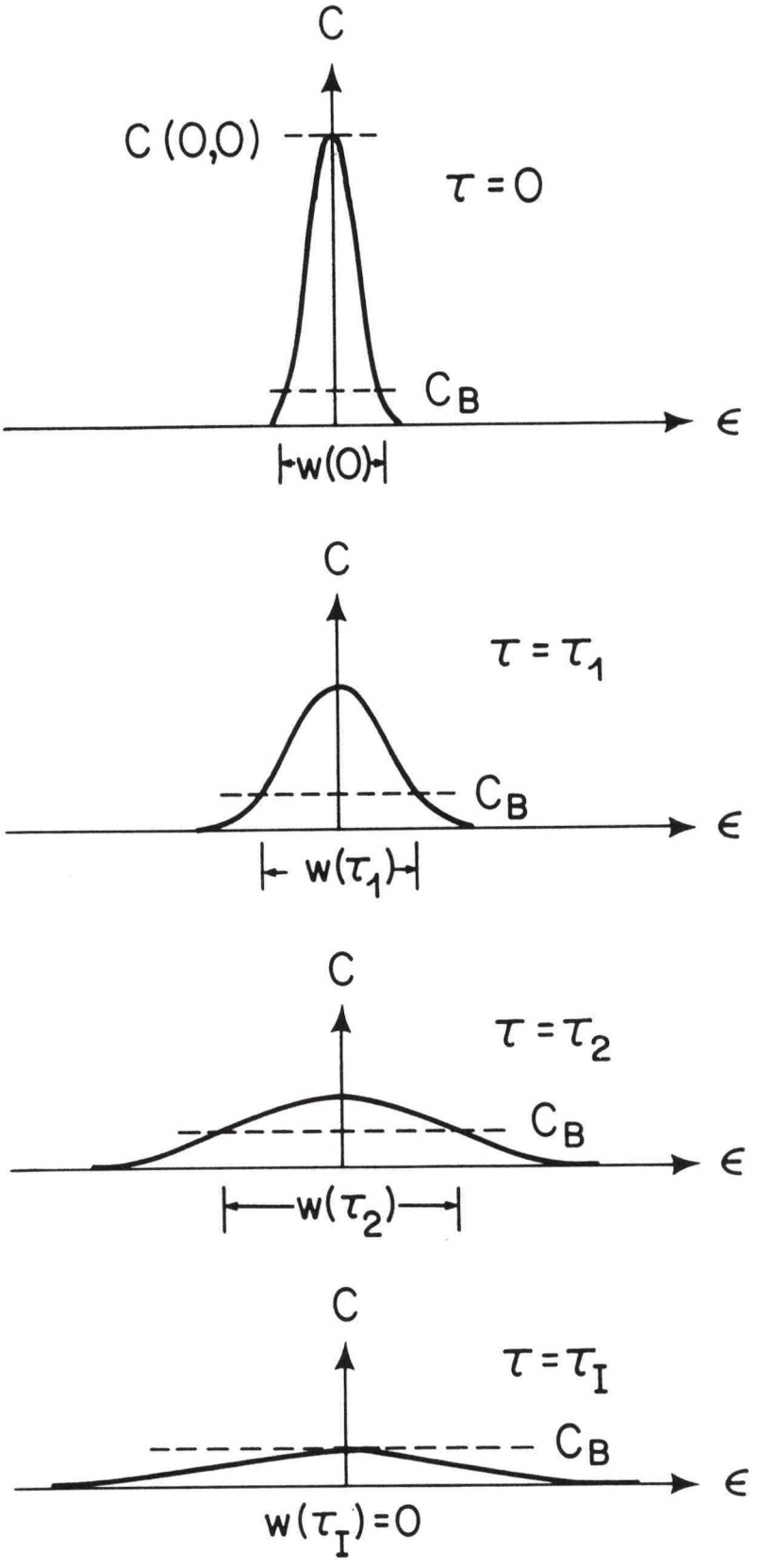

Figure 9. Idealized concentration profiles along a cross-axial plume segment at various times since release. The width, $w(t)$, is defined as the distance over which the concentration exceeds C_B.

where: C_P is the contaminant concentration (relative to the background concentration) along a plume segment of age t (time since release) oriented perpendicular to the plume axis, ε is the distance along the segment, $\sigma(t)$ is the standard deviation of the concentration distribution, and Q is the total contaminant mass per unit area initially in the segment:

$$Q = \int_{-\infty}^{\infty} C_P(\varepsilon, 0) d\varepsilon. \tag{10}$$

For barge discharge, Q can be related to the plume depth, D_P, barge speed, V, and typical contaminant discharge rate from a single barge, m_1, through

$$Q = \frac{m_1}{V\ D_P} \tag{11}$$

Loss of contaminant mass from the plume, which is assumed to be confined to a surface layer of thickness D_P, due to particle settling is accounted for by $F(t)$. The effect of horizontal mixing is dealt with by parameterizing the characteristic growth rate of $\sigma(t)$. Based on dye diffusion studies reported by Okubo *et al.* (1983) and Kullenberg (1982), Churchill (1987) assumed that $\sigma(t)$ grew at a steady rate according to

$$\sigma(t) = \sigma(0) + \omega_D t \tag{12}$$

where ω_D is usually termed the diffusion velocity.

The plume boundaries (where $C_P = C_B$) are at $\varepsilon = \pm\varepsilon_B(t)$, where $\varepsilon_B(t)$ satisfies

$$C_B = \frac{Q\ F(t)}{\sqrt{2\pi}\sigma(t)} \exp[-\varepsilon_B^2(t)/2\sigma^2(t)], \tag{13}$$

Referring to Figure 9, it is easily realized that

$$w(t) = 2\varepsilon_B(t), \tag{14}$$

Determining the detection frequency of discharged lead involved solving (11)–(14) for $w(t)$ [see Churchill (1987) for method of solution] and then using this function in evaluating (2). Computation of $w(t)$ required specifying C_B, V, D_P, m_1, $F(t)$, $w(0)$ and ω_D. C_B was set to a conservatively low value of 25 ng/l, which as noted above is the approximate background level of lead in near-surface slope water. $F(t)$ was determined as described in Section 3.2. Based on the discussion above, V, D_P, $m_{1,Pb}$ and $w(0)$ were set to 3 m s^{-1}, 20 m, 4.5 g s^{-1} and 100 m, respectively. Two values of ω_D were employed: 0.3 and 0.7 cm s^{-1}. Based on the dye diffusion studies mentioned above, these were chosen to characterize horizontal mixing during the stratified and unstratified seasons, respectively. Resulting functions of $w(t)$, for the stratified and unstratified season, are displayed in Figure 10. Note that $w(t)$ for the stratified season reaches a maximum value of roughly 1 km at t=42 hr and shrinks

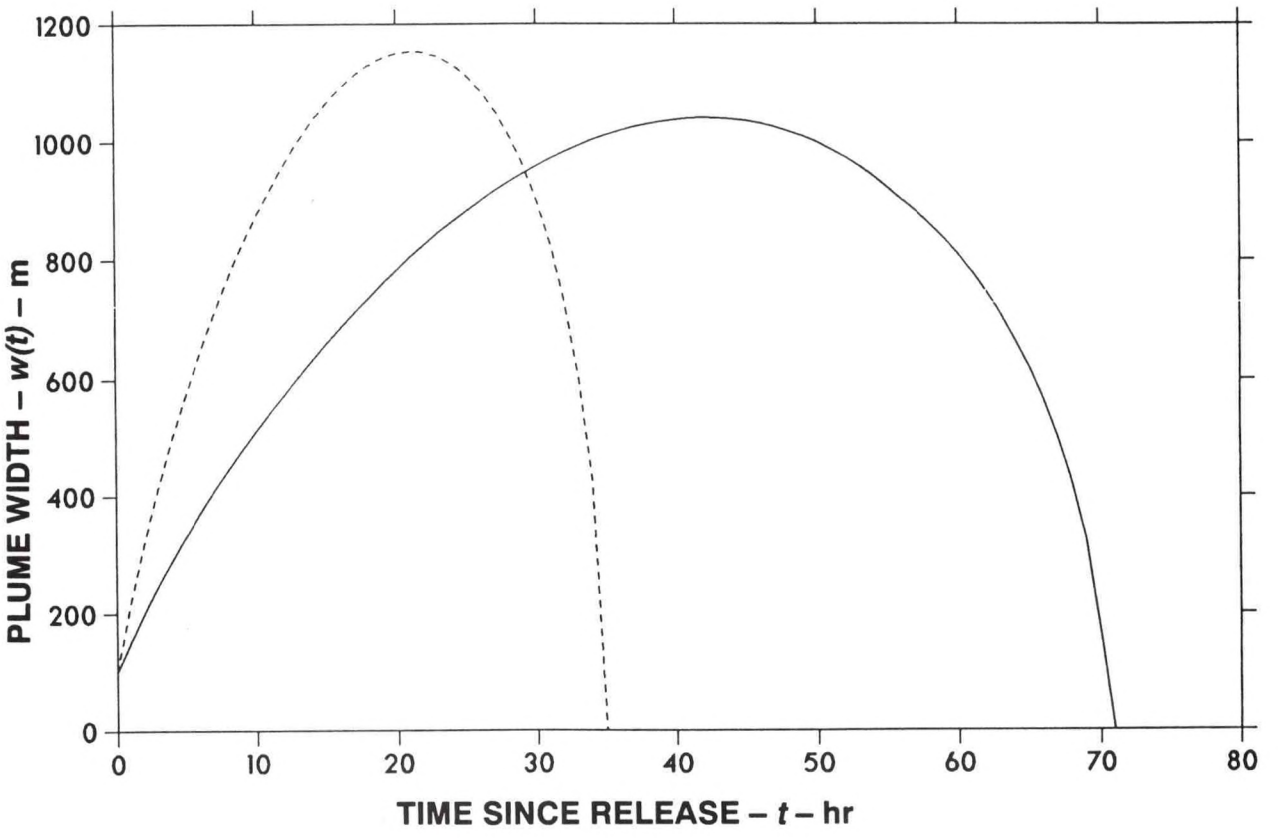

Figure 10. Plume width versus time after release computed by eqns. (11)-(14). The solid [dashed] line was determined with ω_D set to 0.3 [0.7] cm s^{-1} and is deemed characteristic of plume width evolution during the stratified [unstratified] season.

to zero at t=71 hr. This time of zero $w(t)$ is set to T_D when evaluating (2) [see Figure 9]. $w(t)$ for the unstratified season exhibits much the same behavior except that its maximum and zero values occur at $t = 21$ and 35 hr, respectively. These functions compare favorably with observations of sludge plumes formed by discharge at the 106-Mile Site. For example, sludge plumes tracked during September 1987 and September 1988 grew approximately from 100 to 500 m during the first 6 hr after release (Battelle, 1988a, 1989), in close agreement with the growth rate of $w(t)$ for the stratified season. Similar agreement is found comparing $w(t)$ for the unstratified season with the widths of a plume examined in March 1988, which extended to ~600 m at 3 hr after release (Battelle, 1988b). In addition, the maximum age of lead detectability during the stratified season is consistent with "far field" sewage plume observations made in October 1989. During this time sludge with heavy metal concentrations well above background levels was encountered at a site 40 km southwest of the dumpsite (Battelle, 1990). Currents measured during this period were to the southwest at roughly 22 cm s^{-1}, indicating the material had been released roughly 2 days before detection.

Figures 11 and 12 show predicted fields of discharged lead detection frequency during the stratified and unstratified seasons. These were computed using the $w(t)$ functions shown in Figure 10, and with velocity data measured at the MASAR northern mooring line during 15 April–1 September 1984 (for the stratified season field) and 1 December 1984–1 April 1985 (for the unstratified season field). Both fields show a region of relatively frequent lead detection (>30% of the time) over a region extending 10–15 km west of the 106-Mile Site. Both also indicate virtually zero probability of detecting discharged lead at the shelf-edge and upper slope.

Taken together, the results presented in this section indicate that sludge dumping at the 106-Mile Site should have no appreciable effect on lead concentrations at the upper slope and shelf-edge. This is true when considering both the long-term mean concentration and short-term increases in concentration. Additional analysis, not shown here, reveal that this conclusion applies to all other heavy metals contained in sludge released at the 106-Mile Site.

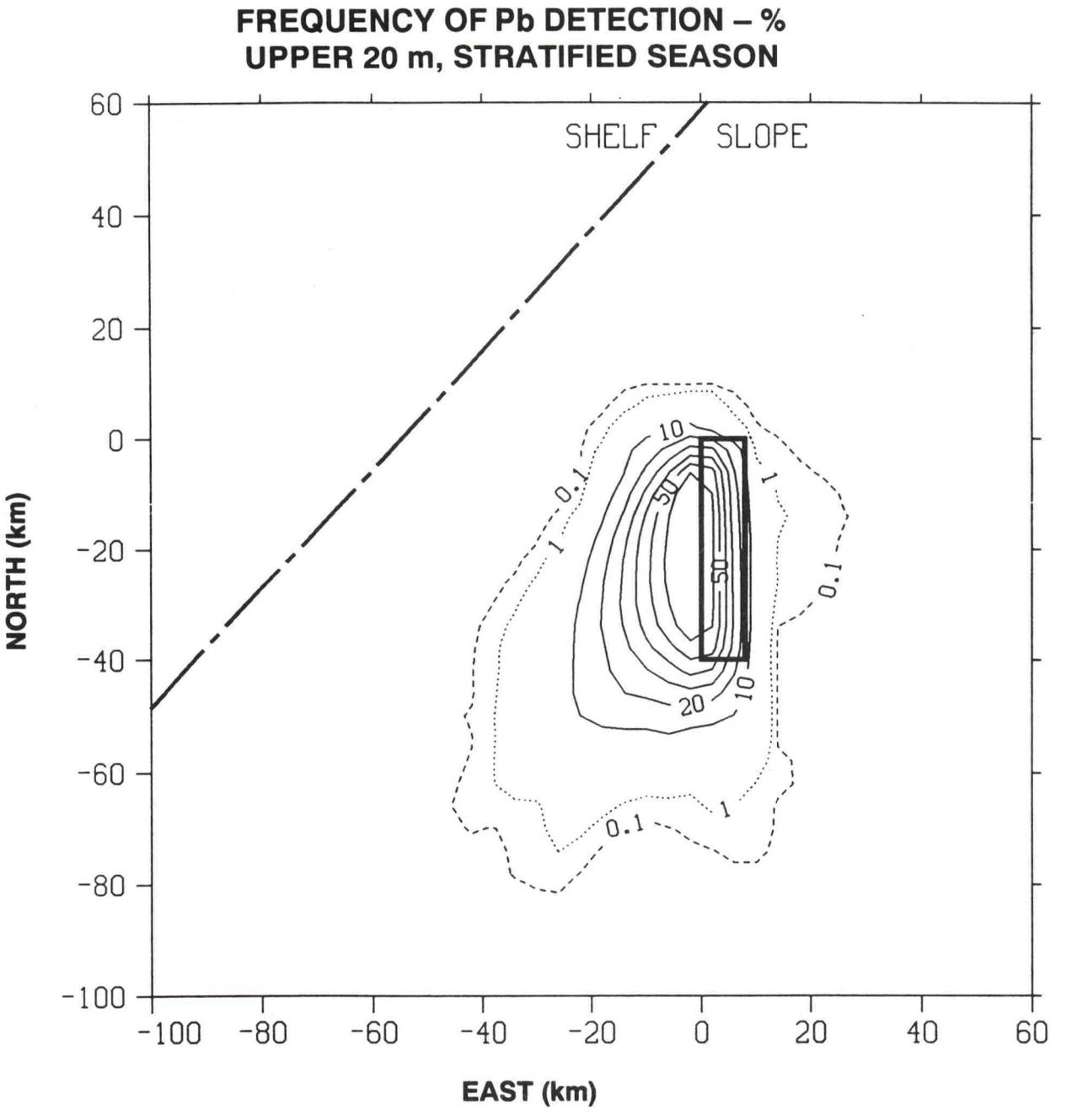

Figure 11. The estimated frequency (%) at which lead discharged at the 106-Mile Site is expected to be detectable within the surface 20 m during the stratified season. The field was computed according to (2) using the solid-line plume width function shown in Figure 10 for $w(t)$ and using velocity data collected during the period of 15 April-1 September 1984 from current meters set at 45-70 m depth on MASAR moorings A, B, and E (Figure 1).

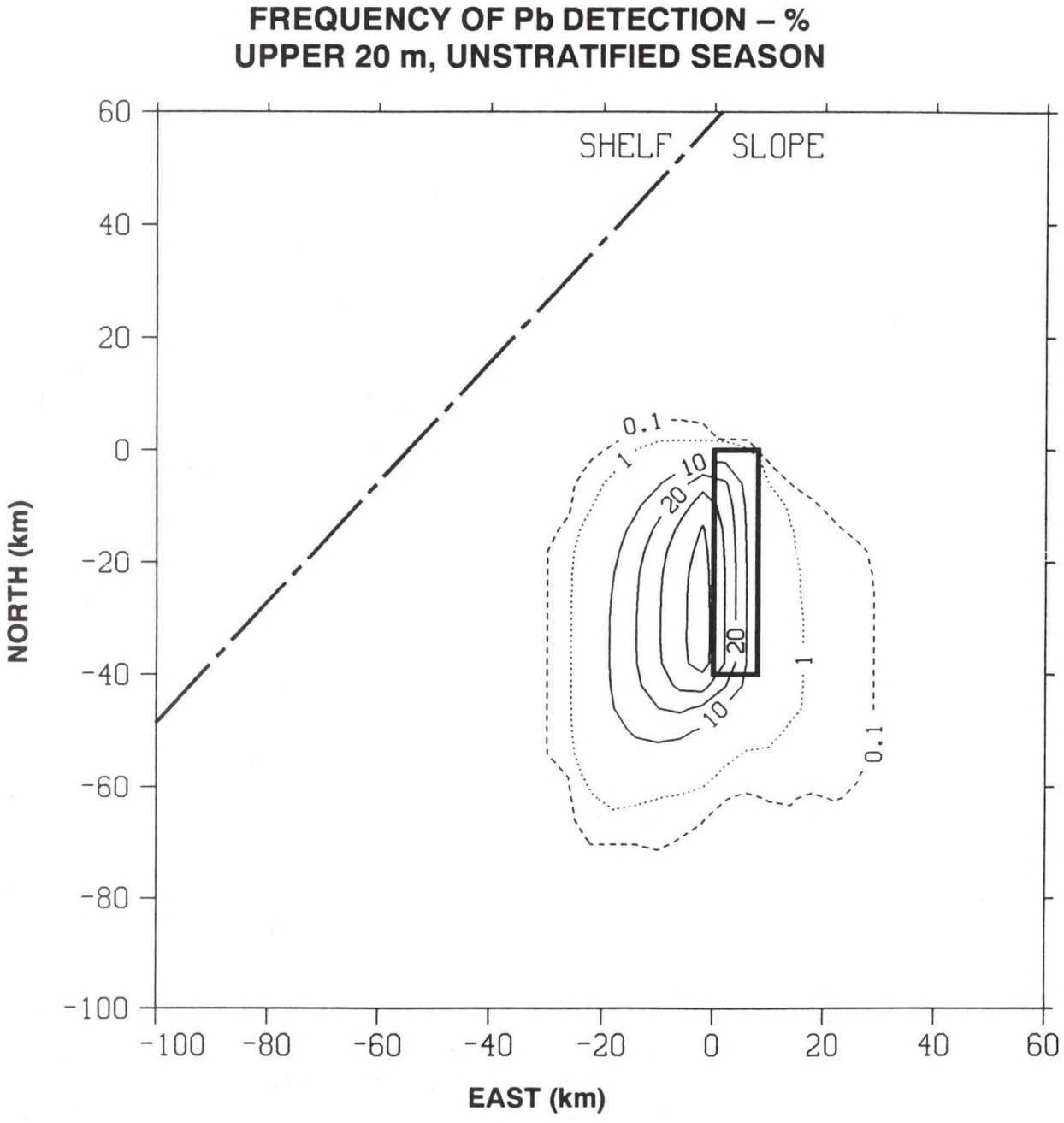

Figure 12. The estimated frequency (%) at which lead discharged at the 106-Mile Site is expected to be detectable within the surface 20 m during the unstratified season. The field was computed according to (2) using the dashed-line plume width function shown in Figure 10 for $w(t)$ and using velocity data collected during the period of 1 December 1984-1 April 1985 from current meters set at 70-170 m depth on MASAR moorings A, B, and C (Figure 1).

5. TRANSPORT OF SLUDGE TO THE SHELF-EDGE

Although analysis presented in the previous section indicates that sludge released at the 106-Mile Site is not expected to arrive at the continental margin with detectable heavy metal concentrations, it is still of interest to estimate how often this material makes its way, in some form, to the upper slope and shelf of the MAB. This was accomplished by evaluating (2) with T_D set to 10 days, considerably longer than the period over which heavy metals are expected to remain detectable in sludge discharged at the 106-Mile Site.

The nonsynoptic nature of the available data presents a problem in determining P for both the shelf and slope. As noted in Section 2.4, the SEEP-I and MASAR data provide sufficient detail of the flow field over the slope, but do not adequately resolve the complex vertical structure of currents over the shelf and shelf-edge. This structure is well resolved by the SEEP-II current meter data, but these data do not include velocity measurements over the slope. This problem has been dealt with by computing $\gamma(x, 10\ days)$ fields over the shelf and slope separately. The fields over the slope, considered in this section, were determined with SEEP-I and MASAR current meter data. γ fields over the shelf are dealt with in the next section.

Determination of γ over both the shelf and slope regions was done with $w(t)$ set to a function which increased at a steady rate, from $W0$ to $W1$, over the first 36 hr after release and remained constant thereafter. $W1$ is deemed the characteristic long-term plume width. As deduced from (2), the resulting visitation frequencies at points more than 36 hr travel time from the 106-Mile Site (at distances of more than 35 km for typical slope water currents) are proportional to $W1$ (because $P(x_S, x, t) = 0$ at these sites for t<36 hr). This enables easy adjustment of the far-field γ distribution for changes in $W1$. All results shown hereafter were determined with $W0$ and $W1$ set to 100 m and 1 km, respectively

Figures 13 and 14 show slope region $\gamma(x, 10\ days)$ fields of the stratified season. These were computed with velocities measured at 45 to 70 m depths along the northern MASAR mooring line; and measured at 12.5 m depth along the SEEP-I mooring line. A slope region $\gamma(x, 10\ days)$ field of the unstratified season, computed with 70–170 m deep velocity data from the MASAR northern line, is shown in Figure 15. All fields show a sharp decline in γ going shoreward over the upper slope. They also show low visitation frequencies ($\leq$5%) at points on the shelf-edge (note that γ is not contoured over the shelf).

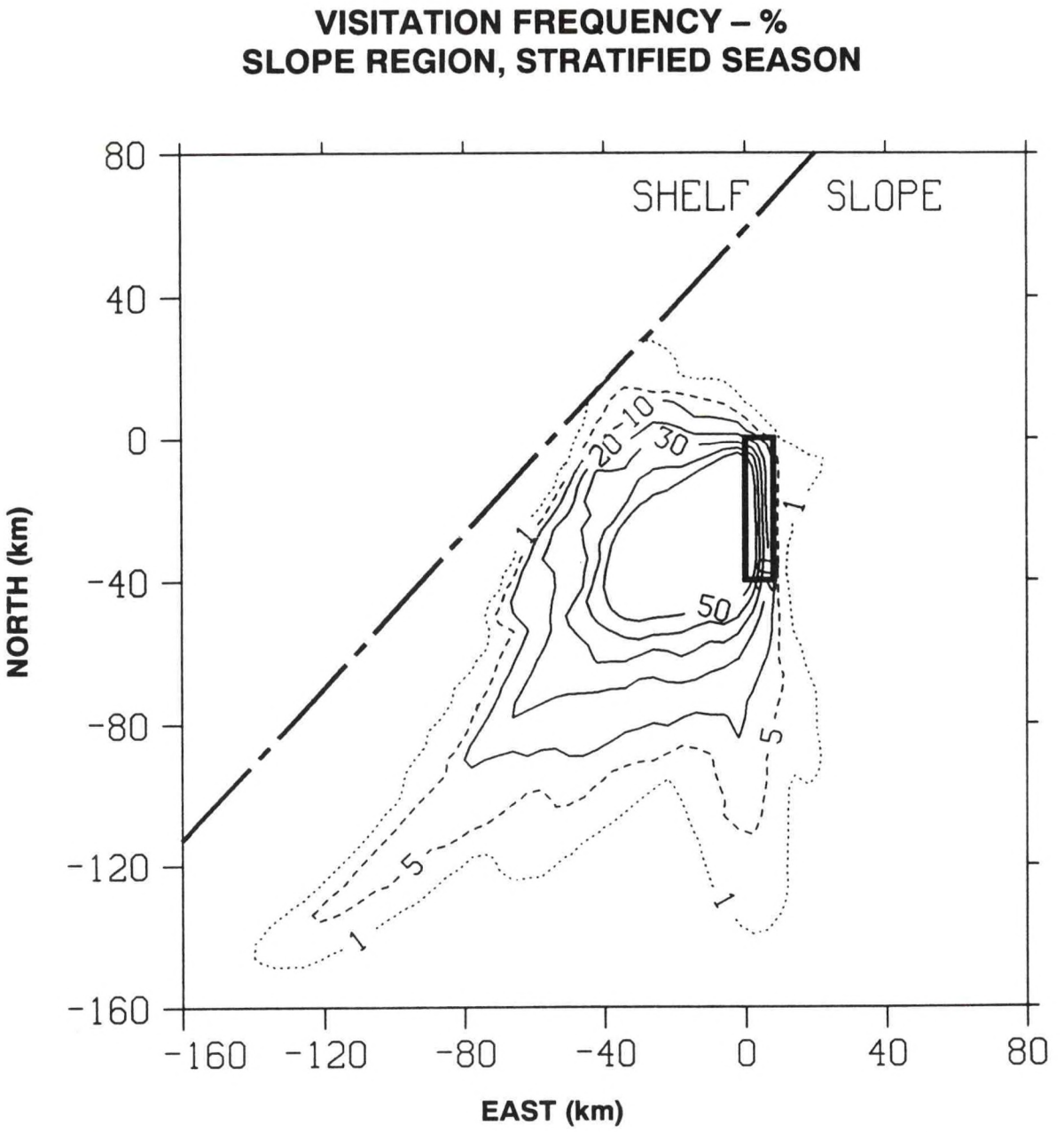

Figure 13. The estimated probability (%) of encountering material discharged at the 106-Mile Site within 10 days after its release, $\gamma(x,10 \text{ days})$, at points over the continental slope during the stratified season. The field was computed using currents measured at 45-70 m depth at moorings A, B, and E of the MASAR northern line during 15 April-1 September 1984. The maximum plume width was set to 1 km.

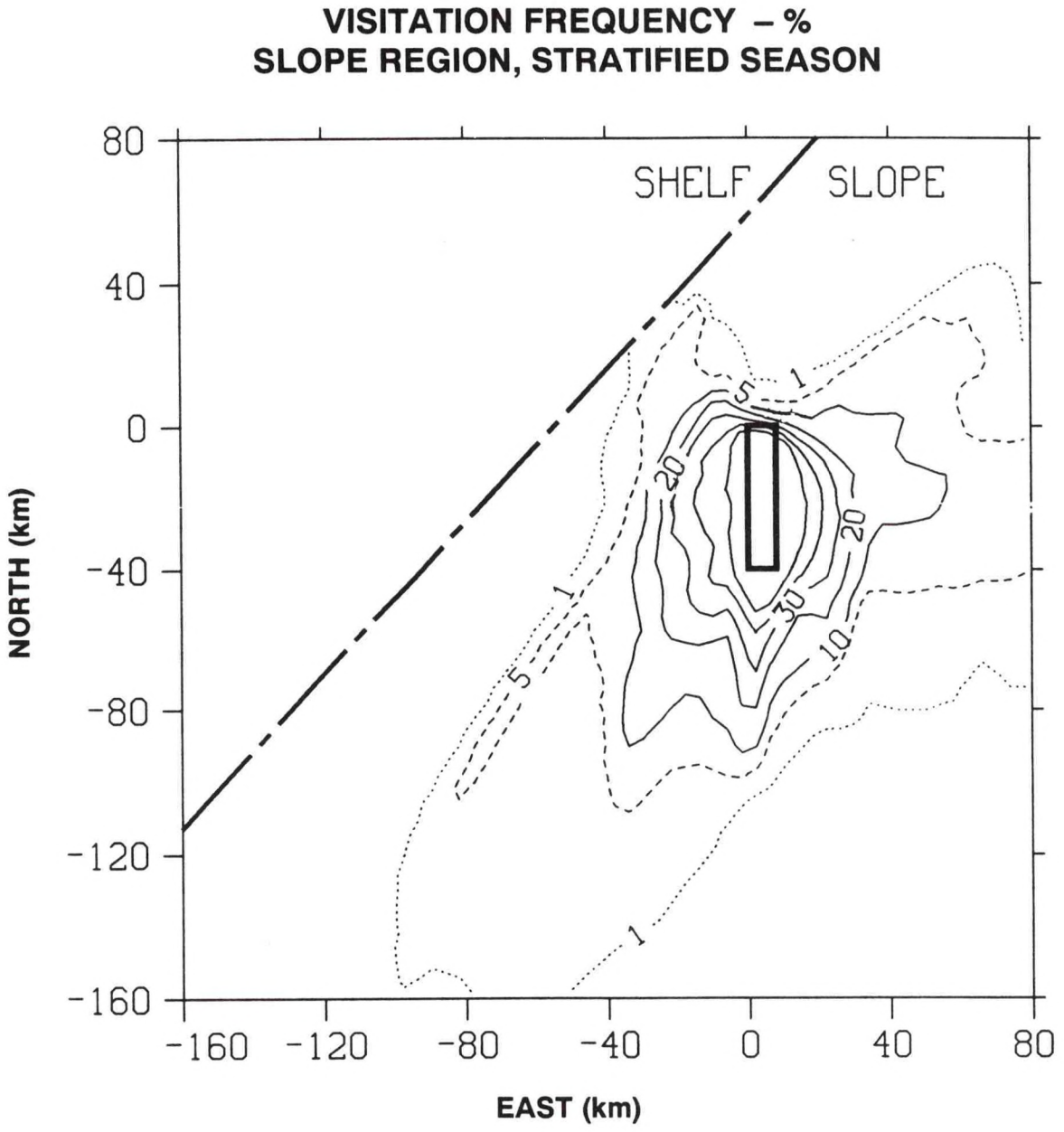

Figure 14. Same as Figure 13 except showing $\gamma(x, 10 \text{ days})$ computed using currents measured at 13 m depth at moorings 1, 2, 3, 4, and 6 of the SEEP-1 line during 1 May-October 1984.

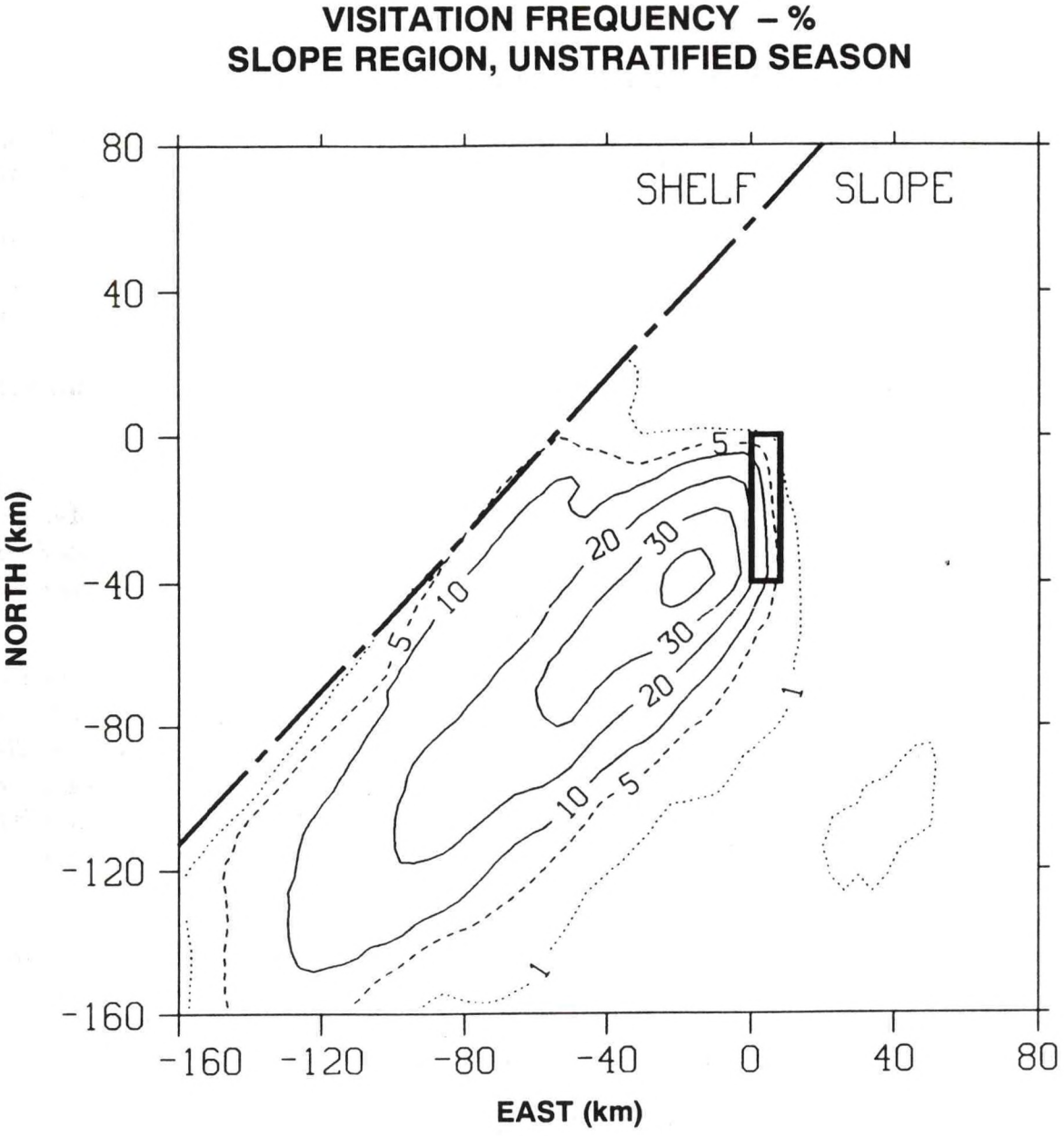

Figure 15. Same as Figure 14 except showing $\gamma(x, 10 \text{ days})$ during the unstratified season as computed using currents measured at 70-170 m depth at moorings A, B, and C of the MASAR northern mooring line during 1 December 1984-1 April 1985.

6. TRANSPORT OF SLUDGE ONTO THE SHELF

The procedure for determining visitation frequency fields over the shelf is derived in Appendix 3. It involves two steps. In the first, slope region velocity data are used to determine the rate at which material from the 106-Mile Site is expected to make its way to the shelf-edge. The subsequent motion of this material is modeled in the second step using velocity measurements from the shelf region. The two steps are coupled with a probability flux function $\xi(x_S, t, x_{SE})$. This function is defined such that $\xi(x_S, t, x_{SE})dx_{SE}$ is the probability per unit of time since release that a water parcel cross a line element, dx_{SE}, centered at x_{SE} at a time, t, following its release at x_S; where, x_{SE} and dx_{SE} are coincident with the shelf-edge.

ξ is determined in the first step by simulating fluid parcel trajectories originating at points, x_S, within the dumpsite and imposing a virtual sink for these trajectories at the shelf-edge. As more fully explained in Appendix 3, ξ is the rate at which trajectories are absorbed by the sink, in units of time since release and distance along the shelf-edge. In essence, $\xi(x_S, t, x_{SE})$ is the flux of $P(x_S, x, t)$ into the virtual sink.

ξ is employed in the second step along with the shelf region velocity data to compute a special version of the visitation frequency. It is designated as γ_{Sh}, and is the visitation frequency of material which has been discharged at the 106-Mile Site and crossed the shelf-edge. A formula for γ_{Sh}, appropriate for the case in which velocity is considered constant along isobaths, is derived in Appendix 3. It is shown below with position represented by Cartesian components of a coordinate system with the x-axis coincident with the shelf-edge:

$$\gamma_{Sh}(\mathrm{x},\mathrm{y},\mathrm{z},T_D) = I\,V\int_0^{T_D} w(t)\int_{-\infty}^{\infty}\int_0^t P_0(\mathrm{x}-\mathrm{x}',\mathrm{y},\mathrm{z},t-t')\varphi(\mathrm{x}',t')dt'dx'dt\ , \qquad (15)$$

where:

$$\varphi(\mathrm{x},t) = \frac{1}{A_S}\int\int_{\mathbf{A_S}} \xi(\mathrm{x_S},\mathrm{y_S},t,\mathrm{x},0)da_S\ ,\ \text{and}$$

$$P_0(\mathrm{x},\mathrm{y},\mathrm{z},t) \equiv P(0,0,\mathrm{z},\mathrm{x},\mathrm{y},\mathrm{z},t)\ .$$

In the above, x=[x,y,z] with y=0 at the shelf-edge, and $x_S = [\mathrm{x_S},\mathrm{y_S},\mathrm{z_S}]$. φ may be viewed as the average ξ for all x_S within the discharge site (it and ξ are considered independent of depth). $P_0(\mathrm{x},\mathrm{y},\mathrm{z},t)$ is the spatial probability density of fluid parcel trajectory endpoints which are confined to a level, z, and originate at [x,y] = [0,0]. Following the method outlined in Section 3.2, P_0 is computed by simulating fluid parcel tracks using shelf region velocity data. γ_{Sh} is taken as the total visitation frequency at points on the shelf.

In evaluating (15) for stratified season conditions, P_0 was estimated using velocity records measured over the period 1 July–18 October 1988 by the ADCP at SEEP-II mooring site 3, on the 90 m isobath (Figure 1). A number of slope water intrusions appeared at the SEEP-II mooring line during this period, as discussed by Flagg *et al.* (1992) and

exemplified by Figure 4. Two versions of φ were computed with stratified season data. One was determined using velocities measured at 45–70 m depth along the MASAR northern mooring line (the same data used to generate Figure 13). The other was calculated with data taken at 13 m depth along the SEEP-I mooring line (also used to create Figure 14). For each version of φ, 17 γ_{Sh} fields were computed. These were spaced at 5 m vertical intervals from 13 to 83 m depth (the ADCP velocity record levels). The fields at each depth were similar (Figures 16 and 17), supporting the assumption that φ does not vary significantly with depth. Consistent with hydrographic observations of slope water intrusions (section 2.2) and the heat flux calculations of Houghton *et al.* (1992), the γ_{Sh} fields showed a maximum tendency for onshelf sludge intrusion within the depth range of 23–43 m, which is typically occupied by the seasonal pynocline during the stratified season.

γ_{Sh} fields of the unstratified season were computed using current meter data collected along the northern MASAR line during 1 December 1984–1 April 1985 to determine φ (also used to generate Figure 15) and velocity records measured over the period 20 February–1 May 1988 by ADCP's at SEEP-II mooring sites 2 and 3 (at the 60 and 90 m isobaths) to compute P_0. These fields showed the greatest tendency of onshore sludge motion near the middle of the shelf water column. A sample field at 38 m is shown in Figure 18. Note that the γ_{Sh} contours of this field extend over greater alongshore distances than the same contours of the stratified season fields of Figures 16 and 17. This is due to differences in the slope region data used to calculate these fields. The data used in creating Figure 18 predicted more rapid and far reaching transport from the 106-Mile Site to the shelf-edge than predicted by the slope region data used in generating Figures 16 and 17 (this difference is also indicated by the γ fields of Figures 13–15). Whether this difference is an actual seasonal trend or an artifact of the particular data sets employed is not known.

All of the γ_{Sh} fields indicate that within the first 10 days after its discharge, sewage from the 106-Mile Site should appear very infrequently, $< 0.01\%$ of the time, at points more than 12 km shoreward of the shelf-edge. It is worth noting that even if the long-term plume width, $W1$, were increased from 1 to 10 km (a reasonable upper limit), $\gamma(x, 10\ days)$ would still be no greater than 0.1% at points 12 km or more shoreward of the shelf-edge.

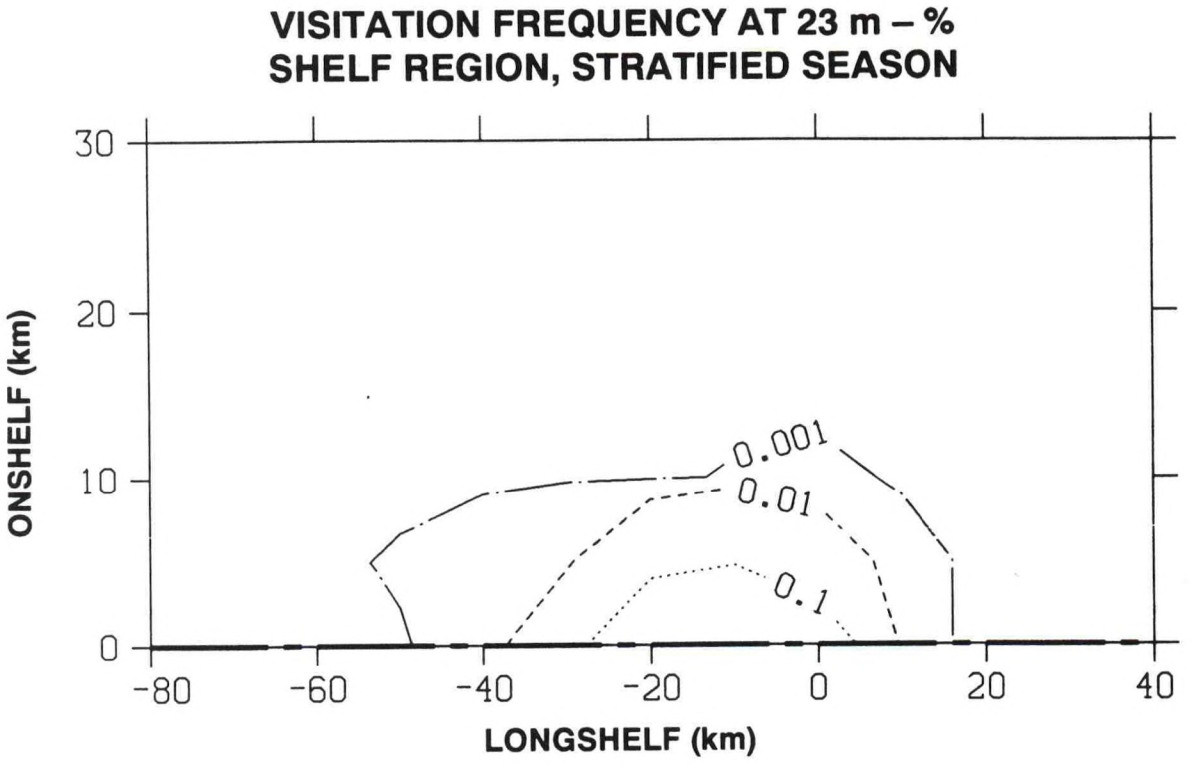

Figure 16. The estimated probability (%) that material discharged at the 106-Mile Site appears within 10 days after its release at points 23 m deep over the continental shelf during the stratified season [i.e., γ_{Sh}(x,y, 23m, 10 days). The onshelf=0 line coincides with the shelf-edge. The field was computed according to (15) using currents measured at 45-70 m depth on MASAR moorings A, B, and E line during 15 April-1 September 1984 to determine ξ and currents measured at SEEP-II mooring 3 during 1 July-1 October 1988 to determine P_0.

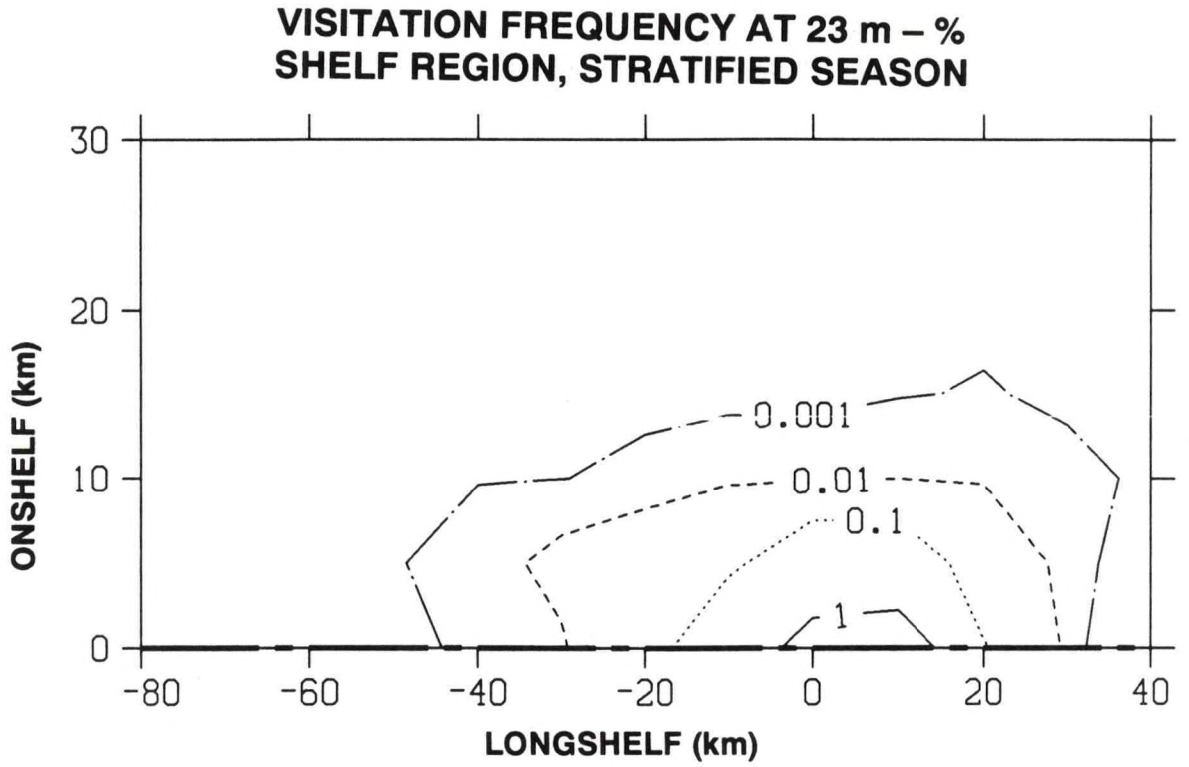

Figure 17. Same as Figure 16 except that ξ was determined with currents measured at 13 m depth at SEEP-I moorings 1, 2, 3, 4, and 6 during 1 May-1 October 1984.

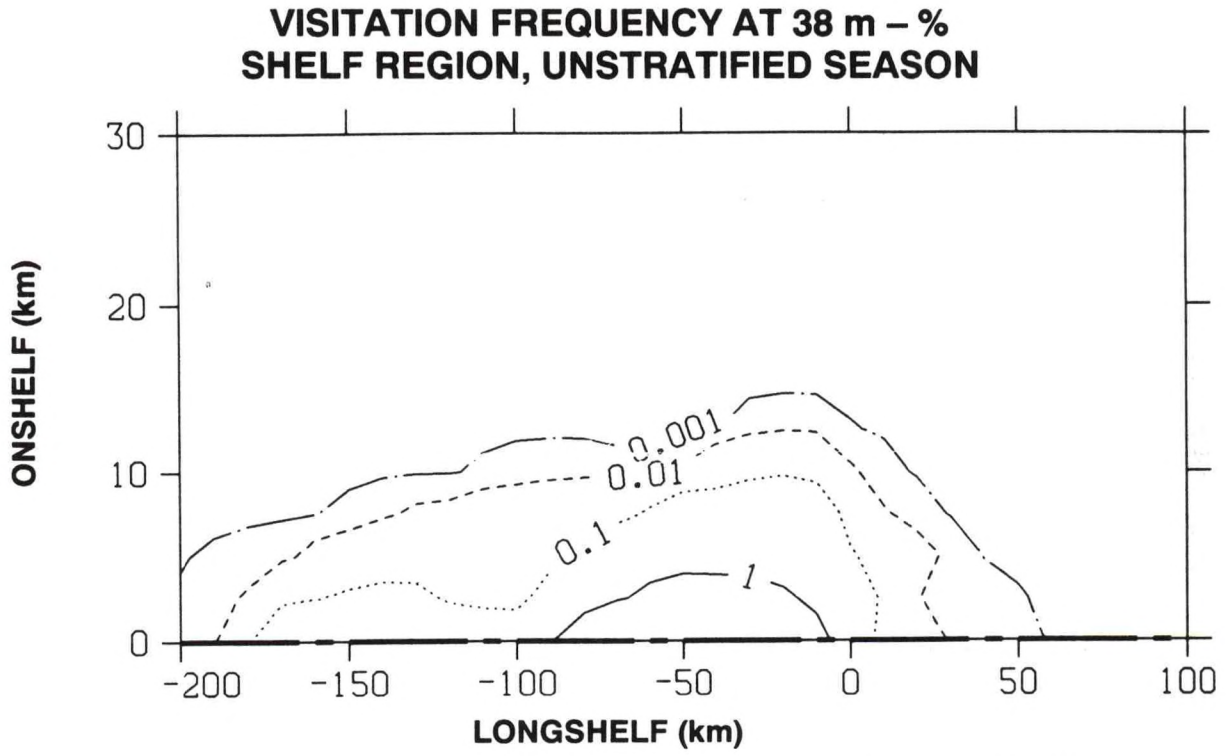

Figure 18. The estimated probability (%) that material discharged at the 106-Mile Site appears within 10 days after its release at points 38 m deep over the continental shelf during the unstratified season [i.e., γsh (x, y, 38m, 10 days). The field was computed using currents measured at 70-170 m depth on MASAR moorings A, B, and C during 1 December 1984-1 April 1985 to determine ξ and currents measured at SEEP-II moorings 2 and 3 during 20 February-1 May 1988 to determine P_o.

7. FRACTION OF DISCHARGED MATERIAL FOUND OVER THE SHELF

A property of interest is the fraction of discharged material which is expected to be found over the shelf within a given time since release. It is difficult to determine this with an acceptable degree of confidence because of the uncertainty in modeling vertical sludge movement over long times since release. For this reason, a proxy has been determined which does not require modeling vertical sludge motion. It is the fraction of material which one would expect to find over the shelf within a given time since release if it were discharged within the 106-Mile Site at a particular depth and remained confined to this level. Denoting this fraction as R and the sludge concentration of this hypothetical situation as C_A, we may write

$$R(z_A, T_D) = \frac{\int\int_{Sh} C_A(x_A, 0, T_D)da}{\int\int_{Sh+Sl} C_A(x_A, 0, T_D)da} , \tag{16}$$

where T_D is the designated time since release, z_A is the mean depth to which sludge is confined, $x_A = [x, y, z_A]$, $\int\int_{Sh+Sl}$ indicates an integral over the area of the slope and shelf (the entire domain where discharged sludge may reside), and $\int\int_{Sh}$ indicates the same type of integral confined to the shelf. Using (3) with $F(t) = 1$ leads to

$$R(z_A, T_D) = \frac{\int\int_{Sh} \int_0^{T_D} \int\int_{A_S} P(x_S, x_A, t)da_S dtda}{\int\int_{Sh+Sl} \int_0^{T_D} \int\int_{A_S} P(x_S, x_A, t)da_S dtda} . \tag{17}$$

It is easily realized that $\int\int_{Sh+Sl} P(x_S, x_A, t)da = 1$, so that the denominator is simply $T_D A_S$. The numerator is determined using the approach described in Section 6 and Appendix 3. Combining (A3.2–A3.9) to give P over the shelf leads to

$$R(z_A, T_D) = \frac{\int_0^{\infty} \int_{-\infty}^{\infty} \int_0^{T_D} \int_{-\infty}^{\infty} \int_0^t P_0(x - x', y, z_A, t - t')\varphi(x', t')dt'dx'dtdxdy}{T_D} , \tag{18}$$

where, as before, a coordinate system with y=0 at the shelf-edge (and y increasing onshore) is used.

Following the method described in Section 6, the above was evaluated by simulating fluid parcel tracks with the velocity data used to generate Figure 16. In simulating tracks over the slope an absorbing boundary, orientated across the slope, was emplaced 200 km southwest of the northeast corner of the 106-Mile Site. This was done to account for the entrainment of slopewater into the northeastward current at the edge of the Gulf Stream (Section 2.4). Resulting estimates of R, valid for the stratified season, are listed in Table 3. Note that R increases with T_D up to T_D=14 days, and remains roughly constant for greater T_D. The maximum R of 0.2 °/₀₀ is at 23 m. Based on this analysis, only a small fraction (order °/₀₀) of the fine-grained material discharged at the 106-Mile Site is expected to make its way to the shelf.

TABLE 3

$R(z_A, T_D)$ for various values of z_A and T_D. $R(z_A, T_D)$ is the fraction of material discharged within the 106-Mile Site which would be expected to reside over the shelf within a time, T_D, after release if it were confined to a depth, z_A. The values listed were computed with the velocity data used to generate Figure 16.

z_A [m]	$R(z_A, T_D)$ [‰]			
	T_D=10 days	12 days	14 days	16 days
13	0.06	0.11	0.15	0.15
23	0.06	0.13	0.19	0.20
33	0.06	0.12	0.17	0.17
43	0.05	0.10	0.14	0.14
53	0.04	0.09	0.12	0.12
63	0.05	0.10	0.13	0.12
73	0.04	0.07	0.09	0.08
83	0.02	0.03	0.03	0.02

8. CONCLUSIONS

The analysis reported on here supports the following conclusions

- Sewage discharged at the 106-Mile Site is not expected to appreciably influence heavy metal concentrations over the shelf or upper slope. More specifically, this material should make a very small contribution to the long-term mean concentration of heavy metals over the shelf and upper slope, and is not expected to arrive at the shelf-edge with detectable heavy metal concentrations.
- The fraction of material discharged at the 106-Mile Site which makes its way to the shelf region is expected to be small, less than one part per thousand based on calculations with stratified season data.
- The discharged sewage which does reach the shelf will be highly diluted and appear at any given point very infrequently (<0.1 % of the time at sites >12 km onshore of the shelf-edge) within the first 10 days after discharge.

It should be emphasized that these conclusions apply for the conditions during which the data employed in this study were collected. One important qualification is that none of the slope region velocity records used were measured in the presence of warm-core rings. Clearly rings will tend to transport material from the 106-Mile Site to the shelf-edge more rapidly than ordinary slope water currents. The frequency at which rings appear at the 106-Mile Site varies significantly from year to year. Sano (1989) reported that warm-core rings passed through the site 24% of the time during 1988. By contrast, only one ring passed through the site during the period of the SEEP-I project, September 1983–October 1984, and it occupied the site for only 4% of this period. No rings were seen at the site during the first 16 months of the MASAR project, March 1984–July 1985.

The influence of rings on sludge transport will be considered in future analysis employing the ARGOS drifter tracks released at the 106-Mile Site (these were not available for the investigation reported on here). A number of these drifters were set out into a ring. The ensemble of drifter tracks will be substituted for simulated fluid parcel trajectories in computing γ and φ. In addition, seasonal γ and γ_{Sh} fields will be calculated using the drifter tracks not released into a ring. A good agreement of these with corresponding fields determined with current meter data will support a number of the assumptions employed in this study (i.e., that P can be adequately determined with current meter data over 200 km longshore distances, and that φ does not appreciable vary over depth and from year to year).

9. ACKNOWLEDGMENTS

Thanks go to Dr. Carlton Hunt of Battelle Ocean Sciences Inc. for helpful advice and for supplying a number of reports prepared by Battelle. Appreciation is also extended to Peter Hamilton of Science Applications International Corporation (SAIC) for supplying the MASAR data set. The MASAR field program was carried out by SAIC through a contract from the U.S. Minerals Management Service

10. REFERENCES

Aikman, F. III, H. W. Ou and R. W. Houghton (1988) Current variability across the New England continental shelf-break and slope. **Continental Shelf Research**, 8, 625–651.

Aikman, F. III and M.B. Empie (1992) Satellite-tracted drifters released across the shelf break in the Middle Atlantic Bight, NOAA Technical Memorandum NOS OES, in preparation.

Battelle (1988a) Final report for nearfield monitoring of sludge plumes at the 106-Mile Deepwater Municipal Sludge Site: Results of a survey conducted August 31 through September 5, 1987. A report submitted to the U. S. Environmental Protection Agency under Contract No. 68-03-3319. Work Assignment 1-63, Battelle Ocean Sciences Inc., Duxbury, MA.

Battelle (1988b) Final report for 106-Mile Deepwater Dumpsite Winter 1988 survey. A report submitted to the U. S. Environmental Protection Agency under Contract No. 68-03-3319. Work Assignment 2-105, Battelle Ocean Sciences Inc., Duxbury, MA.

Battelle (1988c) Characteristics of sewage sludge from the northern New Jersey-New York City area, August 1988. A report submitted to the U. S. Environmental Protection Agency under Contract No. 68-03-3319. Work Assignment 2-111, Battelle Ocean Sciences Inc., Duxbury, MA.

Battelle (1989) Results of the September 1989 EPA survey of the 106-Mile Site. A report submitted to the U. S. Environmental Protection Agency under Contract No. 68-C8-0105. Work Assignment 1-04, Battelle Ocean Sciences Inc., Duxbury, MA.

Battelle (1990) Final report for the 106-Mile Site – October 1989. A report submitted to the U. S. Environmental Protection Agency under Contract No. 68-03-3319. Work Assignment 1-43, Battelle Ocean Sciences Inc., Duxbury, MA.

Battelle (1991) Satellite-tracked surface-layer drifters released at the 106-Mile Site: October 1989 through December 1990. A report submitted to the U. S. Environmental Protection Agency under Contract No. 68-C8-0105. Battelle Ocean Sciences Inc., Duxbury, MA.

Beardsley, R. C., W. C. Boicourt and D. H. Hansen (1976) Physical oceanography of the Middle Atlantic Bight. In: **Middle Atlantic Continental Shelf and New York Bight**, M. G. Gross, editor, **American Society of Limnology and Oceanography, Special Symposia**, Vol. 2, 20–34.

Beardsley, R. C., D. C. Chapman, K. H. Brink, S. R. Ramp and R. Schlitz (1985) The Nantucket shoals flux experiment (NSFE79). Part I: A basic description of the current and temperature variability. **Journal of Physical Oceanography**, 15, 713–748.

Bigelow, H. B. (1933) Studies of waters on the continental shelf, Cape Cod to Chesapeake Bay. 1. The cycle of temperature. **Papers of Physical Oceanography and Meteorology**, 2, 135 pp.

Boicourt, W. C. and P. W. Hacker (1976) Circulation on the Atlantic continental shelf of the United States, Cape May to Cape Hatteras. **Memoires de la Societa Royale des Sciences des Liege**, 10, 187–200.

Bumpus, D. F. (1973) A description of the circulation on the continental shelf of the east coast of the United States. **Progress in Oceanography**, 6, 111–157.

Chapman, D. C. and R. C. Beardsley (1989) A note on the origin of shelf water in the Middle Atlantic Bight. **Journal of Physical Oceanography**, 19, 384–391.

Churchill, J. H. (1985) Properties of flow within the coastal boundary layer off Long Island, New York, **Journal of Physical Oceanography**, 15, 898–916.

Churchill, J. H. (1987) Assessing hazards due to contaminant discharge in coastal waters. **Estuarine, Coastal and Shelf Science**, 24, 225–240.

Churchill, J. H. and P. C. Cornillon (1991a) Water discharged from the Gulf Stream north of Cape Hatteras. **Journal Geophysical Research**, 96, 22227–22243.

Churchill, J. H. and P. C. Cornillon (1991b) Gulf Stream water on the shelf and upper slope north of Cape Hatteras. **Continental Shelf Research**, 11, 409–431.

Churchill, J. H., P. C. Cornillon and G. W. Milkowski (1986) A cyclonic eddy and shelf-slope water exchange associated with a Gulf Stream warm-core ring. **Journal of Geophysical Research**, 91, 9615–9623.

Csanady, G. T. (1980) **Turbulent Diffusion in the Environment**. Reidel, 248 pp.

Csanady, G. T. (1983) Dispersal by randomly varying currents. **Journal of Fluid Mechanics**, 132, 375–394.

Csanady, G. T. and P. Hamilton (1988) Circulation of slopewater. **Continental Shelf Research**, 8, 565–624.

EA Engineering (1991) Wake dilution at the Deepwater Municipal Sewage Sludge Disposal Site bottom-dump and side-dump barges. Final report prepared for the New York City Department of Environmental Protection. EA Engineering, Science and Technology, Inc., 15 Loveton Circle, Sparks, MD.

Flagg, C. N., R. W. Houghton and L. J. Pietrafesa (1992) Summertime thermocline and sub-thermocline cross-frontal intrusions in the Mid-Atlantic Bight. **Continental Shelf Research, in press**

Fornshell, J. A. and W. A. Criess (1979) Anticyclonic eddy observations in the slope water aboard CGC *Evergreen*. **Journal of Physical Oceanography**, 9, 992–1000.

Fry, V. A. and B. Butman (1991) Estimates of the seafloor area impacted by sewage sludge dumped at the 106-Mile Site in the Mid-Atlantic Bight. **Marine Environmental Research**, 31, 145–160.

Gawarkiewicz, G., R. K. McCarthy, K. Barton, A. Masse and T. M. Church (1990) A Gulf Stream-derived pycnocline intrusion on the Middle Atlantic Bight shelf. **Journal of Geophysical Research**, 95, 22305–22313.

Gordon, A. L. and F. Aikman III (1981) Salinity maximum in the pycnocline of the Middle Atlantic Bight. **Limnology and Oceanography**, 26, 123–130.

Hamilton, P. (1987) Current meter measurements at the 106-Mile Site in support of municipal waste disposal. SAIC Report SAIC-87/7541/167. Science Applications International Corporation, Raliegh, NC, 82 pp.

Hay, J. S. and F. Pasquill (1959) Diffusion from a continuous source in relation to the spectrum and scale of turbulence. **Advances in Geophysics**, 6, 345–365.

Hinze, J. O. (1975) **Turbulence**. McGraw-Hill, Inc., 790 pp.

Houghton, R. W. and J. Marra (1983) Physical/Biological structure and exchange across the thermohaline shelf/slope front in the New York Bight. **Journal of Geophysical Research**, 88, 4467–4481.

Houghton, R. W., C. N. Flagg and L. J. Pietrafesa (1992) Shelf-slope water frontal structure, motion and eddy heat flux in the southern Middle Atlantic Bight. **Continental Shelf Research, in press**.

Joyce, T. M. (1984) Velocity and hydrographic structure of a Gulf Stream warm-core ring. **Journal of Physical Oceanography**, 14, 936–947.

Joyce, T. M. and M. A. Kennelly (1985) Upper-ocean velocity structure of Gulf Stream warm-core ring 82B. **Journal of Geophysical Research**, 90, 8839–8844.

Ketchum, B. H. and N. Corwin (1964) The persistence of "winter" water on the continental shelf south of Long Island, New York. **Limnology and Oceanography**, 9, 467–475.

Kullenberg, G. (1982) Physical Processes, In: **Pollutant Transfer and Transport in the Sea, Volume I,** (Kullenberg, G., editor), CRC Press, Boca Raton, Florida, pp. 1–89.

Lavelle, J. W., E. Oztugut, E. T. Baker, D. A. Tennant and S. L. Walker (1988) Settling speeds of sewage sludge in seawater. **Environmental Science and Technology**, 22, 1201–1207.

Lyne, V. D. and G. T. Csanady (1984) A compilation and description of hydrographic transects of the Mid-Atlantic Bight shelf-break front. Woods Hole Oceanographic Institution Technical Report, WHOI-84-19, 290 pp.

Manning, J. and T. Holzwarth (1990) Description of oceanographic conditions on the northeast continental shelf: 1977–1985. NOAA Northeast Fisheries Center Reference Document 90-04, Northeast Fisheries Center, Woods Hole, MA 373 pp.

Mayer, D. A., D. V. Hansen and D. A. Ortman (1979) Long-term current and temperature observations of the middle Atlantic Shelf. **Journal of Geophysical Research**, 84, 1776–1784.

Okubo, A., H. H. Carter, R. E. Wilson, B. G. Sanderson and E. N. Partch (1983) A Lagrangian and Eulerian diffusion study in the coastal surface layer. SUNY Marine Sciences Research Center, Special Report, 46, Reference 83-1, State University of New York, Stony Brook, NY, 295 pp.

Sano, M. A. (1989) Report of water masses receiving wastes from ocean dumping at the 106-Mile Dumpsite, 1 October 1987–30 September 1988 with additional summary for calendar year 1988, NO, NMFS, Document 89-06.

APPENDICES

APPENDIX 1

VISITATION FREQUENCY OF MATERIAL DISCHARGED FROM A MOVING SOURCE

The situation considered here is the discharge of material from a moving source which is confined to a particular region (the 106-Mile Site). What is sought is the proportion of time at which recently discharged material visits a given target site, either inside or outside the disposal area. C83 determined the visitation frequency of material discharged from a fixed source as the probability that a water parcel released at the source pass within a plume radius of a specified target site within a given time after its release. This approach has not proved practicable for the case of a moving source. Instead, the visitation frequency has been derived by considering the ratio of contaminant cloud area to the area of a control region within which the target site is centered. A simple illustration of this approach is provided by considering the probability that a point within a region, **A**, be immersed in a cloud of material of area a which is contained in **A**. If the location of the cloud in **A** is unknown, then the probability is simply a/A, where A is the area of region **A** (this convention is used throughout). Generalizing, we let the area of the cloud change over time according to a function $a(t)$ (which is always much less than A) and introduce a function $p(t)$ which gives the probability that the cloud reside in **A** at a time, t. The stochastic mean probability that points in **A** will be immersed in the cloud over a period T is then $\int_0^T p(t)a(t)dt/AT$.

Returning to the discharge scenario under consideration, let us denote the discharge area as $\mathbf{A_S}$ and specify a characteristic source speed of V. The width of the plume as a function of time since release is denoted by the function $w(t)$. We first consider the visitation frequency of material released into a small area $\mathbf{da_S}$ contained within $\mathbf{A_S}$ and with a center point at x_S. If the discharge is distributed randomly over $\mathbf{A_S}$, then $\mathbf{da_S}$ is filled with material on average once over a period T_R, where

$$T_R = \frac{A_S}{I\, V w(0)}\ , \tag{A1.1}$$

where I is the typical number of individual sources in operation within $\mathbf{A_S}$ at one time (i.e. $I = 2$ if discharge occurs from two sources releasing continuously, or $I = 0.5$ if only a single source is in operation half of the time). The number of times which $\mathbf{da_S}$ is expected to receive material over a sufficiently long period, T, is then

$$n(T) = T/T_R\ . \tag{A1.2}$$

According to the model described above the stochastic mean probability that material released in $\mathbf{da_S}$ arrive at a target site x_F by a time T_D after its release is given by

$$\kappa(x_S, x_f, T_D) = n(T)\ \epsilon(\mathbf{a_f}, \mathbf{da_S}, T_D)/(Ta_f) \tag{A1.3}$$

where $\mathbf{a_f}$ is an area upon which x_f is centered. $\epsilon(\mathbf{a_f}, \mathbf{da_S}, T_D)$ is defined for a single cloud of material deposited at $\mathbf{da_S}$ as the integral over cloud age, to the limit T_D, of the cloud area times the probability that it will reside in $\mathbf{a_f}$ (here we assume that both da_S and a_f are small, but that $da_S << a_f$).

To determine $\epsilon(\mathbf{a_f}, \mathbf{da_S}, T_D)$ we introduce a probability distribution $P(x_1, x_2, t)$ such that $P(x_1, x_2, t)da$ gives the probability that a infinitesimal fluid element released at x_1 will reside in an area da about x_2 by a time t after its release. Because we have stipulated that a_f be small, $P(x_S, x_f, t)$ should be roughly constant over $\mathbf{a_f}$. The probability that a fluid particle released at x_S find itself in $\mathbf{a_f}$ by a time t is then given by

$$\int\int_{\mathbf{a_f}} P(x_S, x, t)da \ \simeq\ a_f P(x_S, x_f, t)\ . \tag{A1.4}$$

To derive an expression for the area of the cloud deposited in $\mathbf{da_S}$ we consider that this and similar clouds deposited in neighboring cells make up a plume element. We stipulate that the size of these clouds always be equivalent and thus, to maintain plume element area, must vary with the size of the plume element. It is reasonable to assume that the plume element's area is a function of its width only, so that the area of the cloud deposited in $\mathbf{da_S}$ is given by

$$a_S(t) = da_S w(t)/w(0) \tag{A1.5}$$

ϵ is then given by

$$\epsilon(\mathbf{a_f}, \mathbf{da_S}, T_D) = \frac{da_S a_f}{w(0)} \int_0^{T_D} w(t) P(x_S, x_f, t)dt \tag{A1.6}$$

κ then becomes

$$\kappa(x_S, x_f, T_D) = \frac{da_S I\ V}{A_S} \int_0^{T_D} w(t) P(x_S, x_f, t)dt\ . \tag{A1.7}$$

The visitation frequency at x_f, is obtained by integrating κ over the discharge region $\mathbf{A_S}$, giving

$$\gamma(x_f, T_D) = \frac{I\ V}{A_S} \int_0^{T_D} w(t) \int\int_{\mathbf{A_S}} P(x_S, x_f, t)da_S dt \tag{A1.8}$$

where $\gamma(x_f, T_D)$ is the visitation frequency at x_f, i.e. the stochastic mean probability that discharged material will visit x_f by a time T_D after its release.

As a test of the above formula consider the situation in which the discharge occurs in still water and the plumes do not grow. In this case $w(t) = W$ and $P(x_1, x_2, t) = \delta(x_1 - x_2)$, where δ is the delta function. At points within $\mathbf{A_S}$, the above expression for γ reduces to

$$\gamma(x, T_D) = \frac{VWT_DI}{A_S} = \frac{T_D}{T_R} \tag{A1.9}$$

which is consistent with intuition.

APPENDIX 2

MEAN CONCENTRATION OF MATERIAL DISCHARGED FROM A MOVING SOURCE

For discharge from either a fixed or moving source, the stochastic mean concentration at a point x_f of material of age (time since release) less than T_D is given by

$$C(x_f, 0, T_D) = \int_0^{T_D} \phi(x_f, t) c(t) dt \tag{A2.1}$$

where $\phi(x_f, t)$ is the likelihood per unit time since release, t, that discharged material of age t be found at x_f, and $c(t)$ is the expected concentration of such material. If the discharge situation considered is that of a mobile source confined to a specified region, $\mathbf{A_S}$, then it follows from Appendix 1 that

$$\phi(x_f, t) = \frac{I\ V\ w(t)}{A_S} \int\int_{\mathbf{A_S}} P(x_S, x_f, t) da_S \ . \tag{A2.2}$$

For the purpose of this analysis we seek the vertically-averaged mean concentration within a designated layer. $c(t)$ is thus specified as the vertically and horizontally averaged concentration in a plume element of age t confined to this layer. From mass conservation considerations, this is given by

$$c(t) = \frac{F(t)\ m_1}{V\ Dw(t)} \ , \tag{A2.3}$$

where D is the layer thickness, m_1 is the mass rate of discharge from an individual source, and $F(t)$ is the fraction of discharged material expected to reside within the layer at age t. m_1 may be related to a disposal-area discharge rate, m, through

$$m = I m_1 \tag{A2.4}$$

Combining the above four expressions gives

$$C(x_f, 0, T_D) = \frac{m}{A_S D} \int_0^{T_D} F(t) \int\int_{\mathbf{A_S}} P(x_S, x_f, t) da_S dt \ . \tag{A2.5}$$

APPENDIX 3

DETERMINING VISITATION FREQUENCY OVER THE SHELF USING DISJOINTED VELOCITY DATA SETS

Derived here is a method for using separate velocity data sets, one from the slope region and the other from the shelf region, to estimate how frequently material from the 106-Mile Site will appear at points over the shelf. The method is carried out in two steps.

In the first step, slope region velocity data are used to estimate the rate at which fluid trajectories originating at the 106-Mile Site cross the shelf-edge. This is denoted as a function: $\xi(x_S, t, x_{SE})$, where x_{SE} is a position vector coincident with the shelf-edge. It is defined such that $\xi(x_S, t, x_{SE})dx_{SE}$ is the probability, per unit t, that a fluid trajectory cross a line element between x_{SE} and $x_{SE} + dx_{SE}$ at a time t after beginning at x_S. Estimation of ξ is done by simulating fluid parcel tracks originating at x_S (within the 106-Mile Site) and imposing an absorbing fluid parcel barrier (sink) at the shelf-edge. The rate at which parcels are absorbed at the barrier, per unit t and x_{SE}, determines ξ. For example, consider an ensemble of N fluid parcel tracks originating at x_S. If between times t_1 and t_2 since release, n of these cross a line element of length Δx_{SE} and centered at x_{SE} , then

$$\xi(x_S, t_{1\frac{1}{2}}, x_{SE}) = \frac{n}{N\ \Delta x_{SE} \Delta t}\ , \tag{A3.1}$$

where $\Delta t = t_2 - t_1$ and $t_{1\frac{1}{2}} = (t_2 + t_1)/2$.

In the second step, a special version of visitation frequency is determined. It is designated as γ_{Sh} and is the visitation frequency of material which has been discharged from the 106-Mile Site and crossed the shelf-edge. To derive an expression for γ_{Sh}, a probability distribution P_{Sh} is introduced. This is defined such that $P_{Sh}(x_S, x, t)da$ is the likelihood that a fluid parcel originating at x_S will cross the shelf-edge and then be found in an area da centered at x by a time, t, after leaving x_S. γ_{Sh} is given by substituting P_{Sh} for P in the "ordinary" expression for visitation frequency (A1.8).

Taking $\xi(x_S, t, x_{SE})$ as the rate at which fluid parcels cross the shelf-edge, allows P_{Sh} to be expressed as a double convolution integral:

$$P_{Sh}(x_S, x, t) = \int_{-\infty}^{\infty} \int_0^t \xi(x_S, t', x_{SE}) P(x_{SE}, x, t - t') dt' dx_{SE}\ , \tag{A3.2}$$

where $P(x_{SE}, x, t)$ is a probability distribution of the endpoints of water parcel trajectories which originate at points, x_{SE} on the shelf-edge.

Integrating the above over the discharge region gives

$$\int\int_{A_S} P_{Sh}(x_S, x, t)da_S = \int_{-\infty}^{\infty}\int_0^t P(x_{SE}, x, t-t')\int\int_{A_S} \xi(x_S, t', x_{SE})da_S dt' dx_{SE} \ . \quad \text{(A3.3)}$$

Defining:

$$\beta(x,t) = \frac{1}{A_S}\int\int_{A_S} P_{Sh}(x_S, x, t)da_S \ , \quad \text{(A3.4)}$$

and

$$\varphi(x_{SE}, t) = \frac{1}{A_S}\int\int_{A_S} \xi(x_S, t, x_{SE})da_S \ , \quad \text{(A3.5)}$$

allows (A3.3) to be rewritten as

$$\beta(x,t) = \int_{-\infty}^{\infty}\int_0^t P(x_{SE}, x, t-t')\varphi(x_{SE}, t')dt' dx_{SE} \ . \quad \text{(A3.6)}$$

At this point it is convenient to express position in Cartesian components using a coordinate system with the x-axis coincident with the shelf-edge. φ is then a function of x only (probability of transport from the 106-Mile Site to the shelf-edge is considered independent of depth). In this coordinate system

$$\beta(\mathrm{x},\mathrm{y},\mathrm{z},t) = \int_{-\infty}^{\infty}\int_0^t P(\mathrm{x}',0,\mathrm{z},\mathrm{x},\mathrm{y},\mathrm{z},t-t')\varphi(\mathrm{x}',t')dt'\mathrm{dx}' \ , \quad \text{(A3.7)}$$

where x =[x,y,z].

To simplify the determination of γ_{Sh}, we employ the assumption that water velocity is constant along isobaths (in the x-direction). With this assumption, it follows that

$$P(\mathrm{x}',0,\mathrm{z},\mathrm{x},\mathrm{y},\mathrm{z},t) = P(0,0,\mathrm{z},\mathrm{x}-\mathrm{x}',\mathrm{y},\mathrm{z},t) \ . \quad \text{(A3.8)}$$

A3.7 then becomes

$$\beta(\mathrm{x},\mathrm{y},\mathrm{z},t) = \int_{-\infty}^{\infty}\int_0^t P_0(\mathrm{x}-\mathrm{x}',\mathrm{y},\mathrm{z},t-t')\varphi(\mathrm{x}',t')dt'\mathrm{dx}' \quad [\text{for } vel = fn(\mathrm{y},\mathrm{z},t)] \ , \quad \text{(A3.9)}$$

where:

$$P_0(\mathrm{x},\mathrm{y},\mathrm{z},t) \equiv P(0,0,\mathrm{z},\mathrm{x},\mathrm{y},\mathrm{z},t)$$

Combining A3.3, A3.4, A3.5 and A3.9 and substituting P_{Sh} for P in A1.8 gives, for the case in which velocity is considered constant along isobaths,

$$\gamma_{Sh}(\mathrm{x},\mathrm{y},\mathrm{z},T_D) = V\int_0^{T_D} w(t)\int_{-\infty}^{\infty}\int_0^t P_0(\mathrm{x}-\mathrm{x}',\mathrm{y},\mathrm{z},t-t')\varphi(\mathrm{x}',t')dt'\mathrm{d}\mathrm{x}'dt\ . \qquad \text{(A3.10)}$$

As noted above, γ_{Sh} is the visitation frequency of discharged material which has crossed the shelf-edge. It thus equals the total visitation frequency at points on the shelf. To obtain the total visitation frequency over the slope, one must add γ_{Sh} to the visitation frequency of material that has not crossed the shelf-edge. The latter can be computed using the fluid parcel trajectories created in the first step (i.e. those subject to an abosorbing boundary at the shelf-edge). In evaluating A3.10, φ is taken from the first step and P_0 is determined by simulating fluid parcel tracks originating at the shelf-edge using the shelf region velocity data.

*U.S. G.P.O.:1992-341-834:60071